Mapping the molecular makeup of the inner kinetochore in the slime mould *Dictyostelium discoideum*

Abstract

During cell division in eukaryotes, the separation of duplicated chromosomes into daughter cells is achieved through the attachment of microtubules to the kinetochore, a multi-protein structure located at the centromere of each chromosome. The kinetochore serves as a link between the microtubules and the centromere and ensures that the sister chromatids are evenly distributed between the two daughter cells. Disturbances in this process are involved in the development of cancer. The inner kinetochore in most eukaryotes, including humans, consists of the histone H3 variant CENP-A, the Constitutive Centromere Associated Network (CCAN) and the Chromosomal Passenger Complex (CPC). However, the kinetochore of *Dictyostelium discoideum* exhibits some unique characteristics, including the absence of CENP-C in the CCAN and the presence of a Survivin-like gene with only one helix and no chromatin-binding domains in the CPC. To better understand the kinetochore in this organism, we employed a combination of gene-tagging, mass spectrometry analysis of immunoprecipitation, and high-resolution imaging. We constructed a BioID variant miniTurbo vector to enable proximity-based biotinylation with nuclear proteins, which can be used for biotin pulldowns. Our results confirm the presence and interactions of several inner kinetochore proteins, but do not provide a clear explanation for the absence of CENP-C. The localisation and function of the putative Survivin ortholog remains unknown, and further optimisation of our methods is necessary to fully address these questions.

Aliek Hasperhoven, S3098885
Supervised by: dr. Eelco Tromer, prof. dr. Arjan Kortholt
Department of Cell Biochemistry, University of Groningen
23 December 2022

Table of contents

Introduction

In eukaryotic cells, every cell division duplicated chromosomes must be equally segregated so that both the two forming daughter cells end up with the same genetic material. Errors in this essential process can lead to chromosomal instability and aneuploidy, which are both hallmarks of cancer (Kops et al., 2005). Perhaps not surprising, chromosome segregation must therefore be extensively regulated and is intricately wired at a molecular level.

Each chromosome contains a centromere, a specialised region of the chromatin where the microtubules of the spindle apparatus can attach to pull the two sister chromatids apart. Centromeres are often found at AT-rich regions of chromosomes and are marked in a non-sequence specific and thus epigenetic manner by nucleosomes in which histone H3 has been replaced by a centromere-specific H3 variant CENP-A. A multi-protein structure called the kinetochore is built on top of the CENP-A nucleosomes and it is this molecular machine that facilitates the attachment of spindle microtubules to centromeres.

The kinetochore can be subdivided into two structural parts: (1) the inner kinetochore, which binds to the centromere and (2) the outer kinetochore, to which the microtubules can bind. Figure 1A shows a schematic reconstruction of the proteins that made up the kinetochore in the Last Eukaryotic Common Ancestor (LECA). The outer kinetochore consists of several protein complexes: (1) the microtubule plus-end tracking protein complexes (shown in the top of Figure 1 in blue and red), that act as stabilising factors to the microtubules (Akhmanova & Hoogenraad, 2005), (2) the KMN-network (Cheeseman et al., 2006; Varma & Salmon, 2012), consisting of the Knl1 complex (light blue, Desai et al., 2003), Mis12 complex (green, Kline et al., 2006) and Ndc80 complex (dark red) and (3) the spindle assembly checkpoint (light blue on the right, partly dark blue lined), that gets activated when the spindle is not accurately attached, to prevent uneven chromosome segregation (Warren et al., 2002). These complexes together form the link between the microtubules and the inner kinetochore. Mis12 of the human Mis12 complex has been shown to bind to one of the proteins of the inner kinetochore, CENP-C (Petrovic et al., 2016).

The inner kinetochore consists of CENP-A (yellow ochre in Figure 1), the Chromosomal Passenger Complex (CPC, turquoise) and the multi-subunit Constitutive Centromere Associated Network (CCAN, yellow). Constitutive in this regard means that this complex is permanently present on the centromere, throughout the cell cycle. The CCAN forms a platform for the recruitment of complexes of the outer kinetochore.

Most of what is known about the composition and function of the CCAN comes from the complexes studied in human cells and the budding yeast *Saccharomyces cerevisiae*. The human CCAN consists of CENP-C, and the complexes CENP-HIKM, CENP-LN, CENP-OPQUR, and CENP-TWSX (see Figure 2). The CCAN of budding yeast, called Ctf19 complex, is similar, but is missing CENP-M and CENP-R and additionally contains Nkp1 and Nkp2. The cryo-EM structure of this yeast complex provides insight in the organisation of the different components of the CCAN (Hinshaw & Harrison, 2019; Yan et al., 2019). Additionally, several cryo-EM structures of (parts of) the human CCAN have been published this year (Pesenti et al., 2022; Tian et al., 2022; Yatskevich et al., 2022). Proteins of the CCAN that directly bind to CENP-A are CENP-C and CENP-N. Together, the CCAN functions as a scaffold on the centromere for the other complexes of the kinetochore to build upon in order to properly attach the mitotic spindle.

It is thought that the LECA already had a fully formed kinetochore (Figure 1A), of which most components are conserved in humans and yeast. Over the course of evolution, some of these components were differentially lost in different eukaryotic lineages. An overview of the composition of the kinetochore can be found in Figure 2 (Salas-Leiva et al., 2021; Eelco C Tromer et al., 2019).

CENP-C and CCAN

One protein thought to be essential in the CCAN is CENP-C. In humans and yeast, CENP-C binds to CENP-A to provide a scaffold for other CCAN proteins to bind. Although the exact composition of the CCAN varies among species, bioinformatics gene predictions find orthologs for CENP-C in almost all organisms that contain a CCAN (Figure 2). However, in the slime mould *Dictyostelium discoideum*, no orthologs for CENP-C could be detected, while most of the other components of the CCAN appear to be present. Because of its function as a scaffold for other CCAN proteins and the fact that orthologs are found in so many other organisms, CENP-C's absence is rather peculiar. How should we interpret this absence of CENP-C? We have three hypotheses: (1) The *Dictyostelium* kinetochore has lost CENP-C, (2) Another protein has taken over CENP-C's function, or (3) the bioinformatics methods lack the resolution to detect CENP-C in *Dictyostelium*.

Chromosomal Passenger Complex and Survivin

The Chromosomal Passenger Complex is another complex found at centromeres in most eukaryotic organisms, including *D. discoideum*. Its localization varies throughout the process of

mitosis. Before reaching metaphase, the complex localises to the inner centromere (between two centromeres) to regulate microtubule-kinetochore attachments. At anaphase onset the CPC translocates to the forming central spindle where it aids in the formation of the midzone and finally the cytokinetic cleft that facilitates the fission of two daughter cells in telophase. In animals, the CPC consists of an Aurora-like kinase, INCENP, Borealin and Survivin. In plants, BORR is found instead of Borealin (Komaki et al., 2020), but up until recently, no analogous and/or homologous proteins for Survivin was found. Survivin in animals and fungi consists of a carboxy terminal helical domain that can form a triple helix with Borealin and INCENP, and a Baculovirus IAP Repeat (BIR) domain that binds to phosphorylated threonine in histone H3 (Kelly et al., 2010). Recent analyses (Komaki et al., 2022) showed that plant cells contain a protein with the same helix, but another phosphate-binding domain, a forkhead-associated (FHA) domain. This FHA domain was shown to bind to histone H3 just like the BIR domain in Survivin does. Interestingly, this study suggested that the defining feature of Survivin-like proteins is not the BIR domain, but its helix. Indeed, in certain eukaryotes, among which *D. discoideum*, an orthologous helix-only gene (only 75 amino acids long) is found, without a phosphate-binding domain. This finding suggests that a single domain was likely the ancestral state of Survivin and phosphate-binding domains were recruited in a parallel fashion in different eukaryotic lineages. Does this single helix protein behave like Survivin and BORI in *Dictyostelium?* Does it interact with other members of the CPC? And does it localise at the centromere before anaphase or is it only part of the CPC at the central spindle? Given the apparent similarity between the *Dictyostelium* Survivin candidate and the supposed single helix Survivin gene – answering the questions above might also shed light on the CPC in the LECA.

Dictyostelium discoideum

D. discoideum is a unicellular organism, belonging to the supergroup Amoebozoa, and has been used as a model organism for studying processes such as chemotaxis, phagocytosis and signal transduction (Bozzaro, 2013).   However, whilst being unicellular under normal growth conditions, *Dictyostelium* can form a facultative multicellular state including a fruiting body with which they produce spores in situations of limited or no nutrients in its environment. Its natural habitat is soil, where it feeds mainly on bacteria. In a lab environment, the cells can be grown in liquid shaking cultures, maintained on agar plates or grown directly on plastic petri dishes, either with bacteria or axenically in artificial medium. When grown axenically, the cell cycle of *D. discoideum* is 8-12 hours. M-phase only makes up about fifteen minutes of the cell cycle (Maeda, 1986).

The kinetochore of *D. discoideum* has not been studied extensively, but some components have been identified. CENP-68 is a Csm-1 ortholog, and can be observed at *Dictyostelium* centromeres throughout the cell cycle (Batsios et al., 2019; Samereier, 2011; Schulz et al., 2009). It colocalizes with CENP-A ortholog CenH3/H3v1, which remains attached to the centrosome during interphase, forming a single cluster (Dubin et al., 2010).

In this project, I will study the composition of the CCAN in *D. discoideum* to study how and if a kinetochore can be built and function without CENP-C present. In addition, I will study the location and behaviour of the recently discovered "Survivin-like" gene in *Dictyostelium*.

Results

To study the composition of the kinetochore in *Dictyostelium discoideum*, genes for several putative kinetochore proteins were amplified with PCR and ligated into vectors with two different tags: GFP and miniTurbo. miniTurbo is an improved variant of BirA, an *E. coli* enzyme that biotinylates lysines of proteins in its vicinity, also called proximity-based biotinylation. miniTurbo, like its predecessor BioID, has a labelling radius of around 10 nm (Branon et al., 2018; Kim et al., 2014).

For tagging with GFP, existing *Dictyostelium* plasmids were used: pDK317 for an N-terminal tag and pDM1209 for a C-terminal tag. Proteins tagged with GFP or miniTurbo can be used to study the kinetochore both with immunofluorescence microscopy for localisation and GFP or biotin pulldowns for interactors. To be able to tag proteins with miniTurbo, a novel plasmid was constructed, which can be used for both Gateway cloning and conventional cloning.

Construction of tagging plasmids for CENPs and Survivin

miniTurbo vector

The plasmid was constructed by fusing the ORF for miniTurbo, flanked by 3xNLS (after the linker) and 3xHA (C-terminal), into Gateway vector pDM627. pDM627 was cut open with SpeI, and miniTurbo was cut with SpeI and XbaI, which result in compatible sticky ends. Because this can result in miniTurbo fusing in both orientations, colonies were checked for correct ligation, by restriction with ScaI and agarose gel electrophorese, as shown in Figure 3, and PCR, as shown in Figure 4. Plasmid 1, 3, 7 and 9 show both the expected pattern after restriction, and a band after PCR, which indicates that the miniTurbo gene was inserted in the correct orientation. This was then checked by sequencing the candidates. They were all correct, so one of them was chosen to continue and was named pET17.

A gene of interest can be inserted into this plasmid (Figure 5) to tag it with C-terminal miniTurbo. This can be used to perform BioID experiments with any nuclear protein. Because this vector contains a Gateway cassette (with chloramphenicol resistance and a ccdB gene, flanked by attR sites), it can be used for Gateway cloning, which makes use of attR sites to recombine with attL sites of a gene to be inserted. Alternatively, it can be used for conventional cloning; after restriction with BglII and SpeI, the Gateway cassette will fall out and a fragment with compatible ends can be inserted. This construction helps with selection of successful colonies, even in conventional

cloning; the ccdB gene is lethal for *E.* coli DH5α cells, so incomplete restriction and self-ligation will not result in colonies.

Tagging of kinetochore proteins

The aim was to tag as many kinetochore proteins as possible, to gather several 'perspectives' on the kinetochore and specifically the CCAN. Primers were designed for 17 different genes (Supplement 2), which were used to amplify ORFs from a cDNA bank of mixed life stages of *D. discoideum*. This yielded no result, so three ORFs were ordered as genestrings and amplified with PCR, using mentioned primers. These three ORFs are for CCAN proteins CENP-H and CENP-L and for Mis12-complex component Nnf1.

After PCR of the genes of interest, the products were run on an agarose gel to check for successful PCR (Figure 6). CENP-H is 906 bp, which corresponds to the size of the band on the gel. CENP-L is a little longer with 1329 bp, which also shows up on the gel. The fragment was amplified with both primers for conventional cloning (left) and Gateway cloning (right). Nnf1 is 699 bp, which corresponds to the size of the upper band.

To screen the colonies of pDM1209 ligations with the different genes, a colony PCR was performed. This makes for a quick check before culturing. The result after agarose gel electrophorese is shown in Figure 7. Only a few colonies turned out to be positive: CENP-H.4 and 9, and Nnf1.4, 5, 6 and 7. The plasmids of these colonies were sequenced and CENP-H.4 and Nnf1.4 were chosen to use for transformation into *D. discoideum*.

For the ligation into pET17, the miniTurbo vector, a restriction analysis was done to check for successful ligations in the backbone plasmid (Figure 8A). Figure 8C shows the expected patterns in case of successful ligation. As becomes clear from this figure, only CENP-L.1 was successfully ligated into the miniTurbo vector. This was confirmed after sequencing, so this plasmid was used for transformation into *Dictyostelium*.

The resulting constructs are as follows:

- CENP-H-GFP
- Nnf1-GFP
- CENP-L-miniTurbo.

Survivin

To study the localisation and interactions of proposed 'Survivin', the ORF was ordered and amplified with PCR. Ligation was attempted in three different vectors: N-terminal RFP, N-terminal GFP and C-terminal GFP. Resulting plasmids were tested by restriction with ScaI and visualised on agarose gel (Figure 9). Only all five colonies of N-terminal GFP were successful, of which the first one was sent for sequencing to confirm. The gene was indeed present in the plasmid, without mutations.

Immunofluorescence and immunoprecipitation

The constructed plasmids were transfected into *Dictyostelium* AX2 cells (or AX3 Aurora-RFP in case of GFP-Survivin) to create cell lines expressing different tagged proteins. To verify the successful expression of the protein of interest in these cells, the cells were examined by immunofluorescence microscopy and an SDS-PAGE was performed followed by Western blot.

While immunofluorescence was used to study localisation of tagged proteins, immunoprecipitation was used to study their protein-protein interaction. This can be done with antibodies against GFP attached to magnetic beads, called a GFP-pulldown or GFP-trap, or streptavidin attached to beads to precipitate biotinylated proteins, also called biotin or streptavidin pulldown.

Cells to be used for immunoprecipitation were synchronized by cold treatment and then arrested in prometaphase with nocodazole. Cells were subsequently lysed and centrifuged to obtain a supernatant of soluble proteins. This supernatant is then loaded onto the beads and further processing leads to beads with an enrichment of proteins of interest. These two samples: (1) the supernatant after centrifugation and (2) the beads with proteins bound, were run on an SDS gel and analysed with both Coomassie staining (Figure 15) and Western blot (Figure 16). For the Western blot, both an α-GFP antibody and streptavidin were used to visualise the proteins.

The GFP trap beads and streptavidin beads are then sent to the mass spec facility, where the proteins are digested. The peptides are separated by liquid chromatography and detected with a mass spectrometer. This results in a long list of detected peptides, that can be analysed against a database of known proteins in *D. discoideum* (AX4 genome). A spreadsheet with the complete data of all detected proteins/peptides is attached as Supplement 3.

To qualify which proteins are likely interactors of the tagged protein, one can look at a few different factors. The first is how many unique peptides are found. These are peptides that can only belong to that protein. The second is sequence coverage: the percentage of the protein of which peptides are found in the pulldown. A coverage of 50% means that half of the protein can be accounted for with the detected peptides. A third factor to look at is intensity, which can be defined as the area under the peak of the MS, indicating how strong the signal of the peptides is. All these factors are semi-quantitative; they cannot be used as quantitative measurements, but give an indication of how much of a certain protein is found in the pulldown.

To compare a certain sample with the control, the enrichment can be calculated based on these different factors. In this experiment, the enrichment was calculated relative to all other samples, to filter away as much junk as possible. In most cases here, I have looked at the enrichment based on unique peptides, together with sequence coverage.

CENP-68

Immunofluorescence
As a positive control for our methods we used a cell line expressing GFP-CENP-68 (provided by Ralph Gräf), which is a known kinetochore protein in *Dictyostelium*. We also used it to test the α-CENP68 serum that we received from the Gräf lab. During mitosis, α-CENP-68 and GFP-CENP-68 co-localize in distinct centromeric foci (Figure 10), so we used it as a marker for the kinetochore in our experiments involving other tagged proteins.

Western blot
On the first blot (Figure 14), only a band at the height of free GFP is visible. On the second blot with the samples from the pulldown (Figure 16), no bands are visible, except the same smear that can be observed in the AX2 negative control cell line.

Coomassie stain
On the Coomassie stained gel, no bands are visible in the sample of the beads (Figure 15).

Mass spectrometry
Indeed, MS did not detect any CENP-68, although a few GFP peptides were detected, with a 64,4% sequence coverage. Next to that, when looking at proteins that are enriched relative to the other pulldowns (Supplement 3), mainly ribosome proteins show up, that can be regarded as background, because they are involved in the expression of the tagged protein. Kinetochore proteins Spc24 (Ndc80 complex) and Stu2 (microtubule-associated) are detected, but only with 1 unique peptide, which is also found in the negative control cell lines (Figure 17).

CENP-H

Immunofluorescence
For the CENPH-GFP cell line, no proof could be obtained for the presence of CENPH-GFP by immunofluorescence, as no cells were found with a clear GFP-signal in the nucleus or on kinetochores during mitosis.

Western blot
On the first blot, only a band at the height of free GFP is visible (Figure 14). On the second blot (Figure 16), a very vague band can be seen in the sample of the beads. The height of this band is again around that of free GFP.

Coomassie stain
In the sample of the beads, a few very vague bands can be observed, but there is clearly no enrichment relative to the input (Figure 15).

Mass spectrometry
In the result from the pulldown (Figure 17), CENP-H is most prominently detected, with 12 unique peptides (against 0 in the other pulldowns), although only with a coverage of 26.9%. Furthermore, CENP-K and CENP-I, both members of the CENP-HIKM complex, are enriched in this pulldown, which is expected. Furthermore, several metabolism-related and ribosomal proteins are detected (Supplement 3), which can be regarded as background signal.

Nnf1

Immunofluorescence
With immunofluorescence, some mitotic cells were found with a kinetochore Nnf1-GFP signal, which corresponds to the expected localization of Nnf1 (one is shown in Figure 11). It must be noted that the signal could not be observed in all mitotic cells, which means there is a heterogenous population of cells in our cultures with different expression levels.

Western blot
Like with CENP-68 and CENP-H, in the first blot only a band at the height of free GFP can be observed (Figure 14). There is a smear above that, which could point to cleavage products of Nnf1-GFP, but because the low quality of the blot this is difficult to say. In the blot from the pulldown (Figure 16), there is in the input sample (supernatant) already a visible band, but again with a smear above it. The band is clearly enriched in the beads sample, but the height of this band again indicates free GFP.

Coomassie stain

Similarly to CENP-H-GFP, the Coomassie stained gel shows a few very vague bands, but no clear enrichment (Figure 15).

Mass spectrometry
In the Nnf1-GFP pulldown, the protein with the highest enrichment based on detected unique peptides is Nnf1-GFP itself, which is expected (Figure 17). The second one is Mis12, which is a known interactor of Nnf1, both components of the Mis12 complex. Another component of that complex, Dsn1, is also found in this pulldown. Furthermore, one peptide of Zwint-1 is found, a protein of the Knl1-complex. Next to these kinetochore proteins, a few nuclear pore proteins, as well as actin-related proteins are found, among which Comitin, which is normally found in the Golgi apparatus (Weiner et al., 1993). The coverages of Comitin and actin-binding protein Q54JS9 are relatively high, comparable to those of members of the complex. Q54JS9 is also found in the CENP-H pulldown with coverages similar to those of expected interactors but is absent in the negative control.

CENP-L

Immunofluorescence
To check for both the presence and the efficacy of CENP-L-miniTurbo, cells were treated with biotin and afterwards fixed for immunofluorescence (Figure 12). Because an HA-tag was added to the CENP-L-miniTurbo gene, the expression of the protein could be tested with an α-HA antibody. This can be seen in the second panel from the left (Figure 12A), which shows an increase in signal over background in the nucleus, which is the expected location of CENP-L-miniTurbo. To check for biotinylation of proteins around CENP-L, streptavidin-Alexa488 was used, which can be seen in the third panel from the left in Figure 12A. The polka dot-like pattern throughout the cell can be observed in practically all cells including the negative control (Figure 12B), and could be explained by the presence of endogenously biotinylated proteins in the mitochondria (similarly observed in Chia et al., 2020). A biotin signal in the nucleus, however, was only found in cells tagged with CENP-L-miniTurbo, which indicates that the miniTurbo biotinylation is working. It is however not guaranteed that it is actually attached to CENP-L, because we couldn't find cells with a distinct kinetochore signal.

Western blot
For CENP-L-miniTurbo, several bands on the Western blot would be expected for proteins that were biotinylated by miniTurbo, but no difference is visible between the CENP-L sample and the negative control cell line (Figure 16). We only see a smear of proteins of 70 kDa and above, which is not specific for the CENP-L-miniTurbo cell line.

Coomassie stain
Corresponding to the result of the Western blot, no protein bands can be seen on the Coomassie stained gel (Figure 14).

Mass spectrometry
CENP-L was tagged with miniTurbo, which biotinylates all proteins in its vicinity. It would be expected that it would also biotinylate itself, or at least other CENP-L-miniTurbo molecules. However, in the biotin pulldown, CENP-L nor miniTurbo was found. Some proteins with high numbers of unique peptides and high coverages are streptavidin itself, and some other background proteins that are found in both miniTurbo and biotin control cell lines (Figure 17). Proteins that are different from the negative control are kinetochore proteins MIS18BP and Stu2 (which was also detected in the Nnf1-GFP pulldown) and a few proteins with roles in splicing. The coverages of these proteins are quite low, and because of the absence of CENP-L and miniTurbo itself, these results are regarded as coincidence.

Survivin

Immunofluorescence
Like with the other cell lines, a sample was taken from the synchronized cells to examine with immunofluorescence microscopy. However, many cells were lost in the process and no mitotic cells with a GFP signal could be found. In another sample, from an unsynchronised population, we found one cell with a defined GFP signal (Figure 13). The signal is located in the middle of the mitotic spindle, in a ring-like shape.

Western blot
Like for the other proteins, a band with the height of free GFP was observed on the first blot (Figure 14). An additional band/smear can be observed at the height of GFP-Survivin (~36 kDa), but because of the low quality of the blot, we cannot say with certainty if this indeed corresponds to GFP-Survivin. On the blot of the pulldown (Figure 16), a band of the expected height can be observed in the first sample, but in the final beads sample only a band corresponding to free GFP is visible, suggesting that somewhere in the process of the pulldown or the SDS-PAGE, GFP-Survivin is cleaved.

Coomassie stain
The result of the Coomassie stain is the same as for CENP-H and Nnf1: we see very vague bands, but no enrichment (Figure 15).

Mass spectrometry

In the Survivin pulldown, we find Survivin itself with a coverage of 85,5% (Figure 17), but none of the proteins you would expect to be interactors of Survivin, such as INCENP and Borealin. The only other protein with a high number of unique peptides and considerable coverage is Albumin, a human protein from blood, which certainly implicates contamination.

Discussion

Summary of this project

During this project, various methods were employed to study the molecular makeup of the kinetochore in *Dictyostelium discoideum*, with the aim of explaining its absence of CENP-C and verifying the presence of Survivin as a members of the Chromosomal Passenger Complex. To achieve this goal, several predicted kinetochore proteins were tagged with GFP or miniTurbo (BioID) and expressed from stable episomal vectors. Transformed polycolonal cell lines were analysed using immunofluorescence microscopy (IF) and Western blotting, with varying levels of success. Nonetheless, all engineered cell lines were used for subsequent pulldown experiments, the results of which were analysed using mass spectrometry. Table 1 provides an overview of the outcomes of the different cell lines for each method with respect to observation of the tagged protein.

	IF	Western blot	Mass spec
CENP-68	+	Tag only	Tag only
CENP-H	-	Tag only	++
Nnf1	+	Tag only	++
CENP-L	nuclear	-	-
Survivin	-	+	+

Table 1. Proof of presence of the tagged protein in all cell lines.. For IFA and Western blotting, a "+" indicates that evidence of a successful tag was found, while a "-" indicates that no evidence was found. For mass spectrometry, a "+" indicates that the protein was detected but without interactors, while a "++" indicates that expected interactors were found.

I will first discuss the sometimes-conflicting results that were obtained for each of the different cell lines using the three methods (Table 1). I will specifically focus on factors that should be optimised to obtain reliable results. Then, I will draw minimal conclusions from the presented results, and will discuss their implications for the knowledge on the *Dictyostelium* kinetochore. Finally, I will outline some suggestions for future research.

Optimisation of protocols

Different methods to assess the presence/absence of tagged proteins in our engineered *Dictyostelium* cell lines produced seemingly inconsistent results. Such ambiguity results in an uncertainty regarding the presence of tagged proteins, and hints to some fundamental problems in our protocols. To obtain reliable results in the future, it will be necessary to optimise the protocols used for the experiments described in this report.

Immunofluorescence microscopy
During this project, several immunofluorescence samples were made and examined, but the signal in these different samples was not consistent. In the first stages, the cells often looked better than in later stages, although the same protocol was used every time. Furthermore, our protocols did not produce images of the same resolution and consistency as previously published studies (Samereier, 2011). There are several possible reasons for this. The Triton X-100 that is used to wash and permeabilise the cells, was old, which can lead to it becoming reactive. The mounting medium is also a sensitive aspect: too much will lead to loss of resolution, and too little will cause quicker decay of the fluorophores. Because the samples were imaged a few days after the sample preparation, proper mounting is essential to prevent decay of the fluorophores. Another factor that could be optimised is the fixation method: formaldehyde fixation was chosen instead of (partial/mixed) glutaraldehyde fixation, which is known for optimal microtubule signal, or cold methanol. This was done because autofluorescence of GFP is lost with glutaraldehyde fixation, but this can be rescued by staining with antibodies against GFP. Optimising these factors would lead to better immunofluorescence images, which would take away the uncertainty of whether cell lines were successful and provide more information on localisation of the proteins.

Lysis: residual proteolytic activity and switching to other tags
GFP-CENP-68 was used as a positive control for all our methods, since we knew from previous work that this cell line was constructed properly and showed signal in both IFA and Western blot (Samereier, 2011; Schulz et al., 2009), also a polyclonal antibody for CENP-68 was available to double check our efforts (kind gift from Ralph Gräf). Using Western blot as a readout, only GFP was detected, without CENP-68. In addition, in the CENP-68 pulldown, only free GFP was pulled down with the GFP-Trap beads. For CENP-H and Nnf1, only free GFP was detected by Western blot in both unsynchronized cells (Figure 14) and the samples from the pulldown (Figure 16). Collectively, this likely indicates that the GFP tag is cleaved off the proteins of interest at a particular step in our lysis/pulldown protocols. Because we obtained clear fluorescence signal for GFP-CENP-68 and Nnf1-GFP at the kinetochore in selected cells, it is unlikely that such cleavage

already occurs *in vivo*. However, it is possible that the tagged protein comes into contact with proteases during lysis, and the linker between the tag and the proteins of interest was cleaved. *Dictyostelium* is known to have high proteolytic activity (Schauer et al., 1993). To prevent excessive cleavage of tags, several protease inhibitors (PIs) were added to the lysis buffer. In the lysis buffer for the first blot, an old PI mix was used that may have lost its effectiveness. For the pulldown, a new PI mix was made but was missing one component (N-CBZ-Pro-Ala). Possibly this incomplete PI mix was not sufficient to fully prevent active *Dictyostelium* proteases from cleaving the linker between GFP and CENP-68 (sequence unknown). This same theory may apply to the other proteins where cleavage was observed: CENP-H (linker sequence: ASGGSGGS), Nnf1 (idem), and Survivin (SGLRS).

To prevent unwanted proteolytic cleavages, the lysis protocol should be optimized by finding the optimal pH, salt concentration and detergent (here Triton and NP-40 were used) that results in the lowest protease activity possible without damaging the interactions between the proteins of interest. Keeping the temperature low should also help to limit protease activity as much as possible. Another option is to use a different tag where a linker might not be needed, such as a His tag or a FLAG tag. These tags can also be used for Western blot, immunofluorescence microscopy, and immunoprecipitation (pulldowns), as there are also ample antibodies available for tag-specific detection.

Lysis: prevent loss of interactors
Another reason the lysis protocol should be optimised is to keep protein-protein interactions intact in the lysate for the GFP-pulldown. Especially for GFP-Survivin, where no interactors were found, this factor could be of great importance to gather more knowledge about the protein. Optimisation can be sought in the type and concentration of detergent and salt concentration.

Furthermore, proper breakdown of DNA is needed, as the kinetochore binds to chromatin. After lysis, the lysate is centrifuged and only the supernatant is loaded onto the beads. Bulky chromatin might precipitate with the pellet, and if the proteins of interest are still bound to the chromatin, they will not be able to bind to the beads. In this experiment, sonication was used to shear the chromatin, however this protocol was not optimised, and the pellet was not properly checked with Western blot to verify whether tagged protein was not left in the pellet. Especially for CENP-L-miniTurbo, where neither CENP-L, nor the tag were detected in the pulldown, this could be an explanation. Because streptavidin and biotinylated proteins of the mitochondria were indeed detected, the pulldown itself seemed to have worked, but it is possible that CENP-L-miniTurbo just did not get to the beads as it was spun down.

When the protocol will be optimised, the experiment must be executed in triplo (at least). If proteins show up in all three experiments, coincidence can be ruled out, and statistical analyses can point out significant enrichment compared to a negative control.

An additional control for the GFP pulldown would be a GFP-only or nuclear GFP-only cell line. In this way, proteins that interact with GFP or are involved in its maturation instead of those that interact with the protein of interest can be ruled out as background.

BioID
The BioID/miniTurbo experiment yielded no results, not even CENP-L or miniTurbo itself. As a control, it would be helpful to have a nuclear BioID-only cell line. In this way, all proteins that are in the nucleus and get biotinylated by miniTurbo, but do not necessarily have specific interactions with the protein of interest, can be excluded from the analysis, because they also appear in the BioID-only control. This would also enable detection of successful cell lines by immunofluorescence microscopy, because presumably a difference between just a nuclear signal and a kinetochore signal can be observed in mitotic cells.

In the biotin pulldown, a lot of mitochondrial proteins were detected, which corresponds to the signal observed in immunofluorescence. To exclude this signal from the pulldown, another lysis method can be used, wherein the nucleus is first extracted, before it is lysed to release the nuclear proteins. With this method, it is possible to exclude the incorporation of mitochondrial proteins, preventing the streptavidin from being saturated with these background proteins.

Mass spectrometry
Although the mass spectrometric analysis revealed some expected protein interactors, coverages and numbers of unique peptides detected of some proteins were disappointing. The coverages of interactors are supposed to be between 50 and 80%, usually indicative of good quality of pulldown (correlates with the amount of pulled down protein), which would allow to conclude that these are real interactors. The coverages and intensity values of unique peptide numbers of most of the detected proteins are much lower (for specific interactors the coverages are <20%), especially in the CENP-H pulldown. This makes it difficult to see the difference between specific interactions and the abundant background signal that is present in *Dictyostelium* immunopulldowns. Signal optimisation could be obtained both by having a higher absolute number of cells before lysis, and a relatively higher number of mitotic cells. In other words: improve synchronisation to enrich for mitotic cells. This is particularly relevant for Survivin and

Nnf1, that are thought to only localise to the kinetochore during mitosis, implicating that interesting interactions can only be found in mitotic cells.

Molecular cloning

Because the presence of CENP-L-miniTurbo could not be verified with microscopy and/or Western blot, it would have been possible to also check for the bona fide presence of the vector in our cells lines. PCR on cell lysates with the forward primer of the protein of interest and reverse primer of the tag (in case of a C-terminal tag, vice versa for an N-terminal tag) should give a band for cells where the protein is successfully tagged.

Polyclonal cell lines

To prevent the problem of cell lines where not all cells express the protein (in equal quantities), more attention should be given to formation of monoclonal cell lines. This can be done by choosing only one colony after growing out successful transfectants and culturing the cells as short as possible, before they have the chance to develop mutations. More cells expressing the tagged protein will naturally lead to a better signal. A better option could be to tag the endogenous locus instead of using an overexpression plasmid. A technique to accomplish this is CRISPR/Cas9, which allows to make changes directly at the level of the genomic DNA. Using this technique, it would be possible to acquire cell lines where 100% of the cells express the tag, in addition to eliminating problems of overexpression. Although standard CRISPR/Cas9 techniques make use of a NGG PAM site, which is difficult to find in *Dictyostelium*'s AT-rich genome, several Cas9 orthologs have been discovered that allow for the use of this technique in *D. discoideum* (Yamashita et al., 2021).

Cell cycle synchronisation

Another factor that majorly complicated this study, is the low number of mitotic cells in normal populations and the difficulty of synchronising the cell cycles to enrich for mitotic cells. The cultivation of cells on bacteria as opposed to axenic media has been shown to reduce the duration of the cell cycle (Pears & Gross, 2021). However, the removal of bacteria during analysis of the cells introduces additional difficulties. The method I used to introduce synchrony is a combination of cold treatment, where the cells are kept below 11,5°C for 20 hours to arrest them in G_2 phase (Maeda, 1986), and nocodazole, a microtubule depolymerizing drug that prevents spindle formation and thus arrest cells in prometaphase (Welker & Williams, 1980). After cold treatment, cells were brought to 22°C to allow them to leave G_2 phase and nocodazole was then added to prevent them from continuing and leaving M-phase. Because nocodazole prevents spindle formation, it is difficult to identify mitotic cells with fluorescence microscopy, thus we did not test if our method worked and if mitotic enrichment was achieved. An alternative would be to use

Fluorescence Activated Cell Sorting (FACS) to sort out mitotic cells after they have been fixed, with the help of antibodies against specific mitotic markers (Zhu, 2012).

Another drug that can be used to induce mitotic arrest is Taxol, which stabilises the mitotic spindle by preventing microtubule degradation (Xiao et al., 2006). Because Taxol halts mitosis after the assembly of the mitotic spindle, this makes it easier to identify mitotic cells by microscopy. A genetic 'trick' to halt cells in mitosis is to introduce a gene for non-degradable cyclinB with an inducible promotor, which will keep Cdk1 active, prohibiting the cells to leave M-phase (Luo et al., 1994).

Some of thes mentioned methods can be combined, but finding the ideal circumstances requires thorough optimisation.

Implications and suggestions

Although most of the obtained results are not of the desired quality, some preliminary conclusions can be drawn.

Nnf1
According to immunofluorescence microscopy, Nnf1-GFP localises to the kinetochore. The pulldown shows that it interacts with Mis12 and Dsn1. Furthermore, ZWINT-1 was found, which is part of the Knl-1 complex and directly interacts with the Mis12 complex in model eukaryotes (Petrovic et al., 2016). These results indicate that the predicted genes for Nnf1, Mis12 and Dsn1 indeed code for kinetochore proteins, specifically components of the Mis12 complex, and that this complex interacts with the Knl-1 complex, similarly to the kinetochore in humans and yeast (Kline et al., 2006; Petrovic et al., 2016). We did not identify the fourth component of the Mis12 complex Nsl1. Since Nsl1's direct binding partner Dsn1 was also only identified with 2 unique peptides, we reckon Nsl1 might have well been below our detection limit or specific peptide of Nsl1 are not optimally detected by mass spectrometry for other reasons (e.g. due to unknown modifications at the peptide level).

CENP-H
Although CENP-H-GFP could not be observed at the kinetochore in immunofluorescence microscopy, mass spectrometric analysis of GFP pulldown experiments show interactions with CENP-I and CENP-K. These proteins are expected to be part of the CENP-HIKM complex at the kinetochore (Yatskevich et al., 2022), which confirms the gene predictions of both CENP-H, and CENP-I and CENP-K. However, no further interactions could be observed, this either means that the CENP-HIKM complex might have another role at the chromatin in *Dictyostelium* or our

pulldown/lysis conditions need to be further optimised to enrich for additional interactors. One such optimisation can be sought in using cross-linking agents such as paraformaldehyde, which is now an established method to for proximity proteomics apart from BioID (Brusini et al., 2022).

Absence of CENP-C

Although our pulldown experiments confirm the presence of canonical subcomplexes within the kinetochore of *Dictyostelium*, none of the three hypotheses that explain CENP-C's apparent absence could be confirmed.

The first hypothesis, that the *Dictyostelium* kinetochore has lost CENP-C, would be probable when we would have found all other inner kinetochore proteins except CENP-C. We would then expect another protein, like CENP-N, to bind to CENP-A. Further interaction studies of CENP-N would clarify this. The second hypothesis, that another protein, that is not an ortholog of any known kinetochore proteins, has taken over the function of CENP-C, would be likely if both the CENP-H-GFP and biotin pulldown of CENP-L-miniTurbo, and possibly the Nnf1-GFP pulldown would surface a protein of previously unknown function, or a protein which presence cannot be explained in another way. Since we did not find such a protein, we cannot corroborate this hypothesis. The third hypothesis, that the *Dictyostelium* kinetochore is indeed functionally and molecularly analogous to the human CCAN, implies that CENP-C binds to the CENP-HIKM complex through a combined surface of CENP-H, K and M (Yatskevich et al., 2022). In this scenario CENP-C is expected to appear a fully optimised pulldown of for instance CENP-H, which would allow us to draw the conclusion that *Dictyostelium* indeed possesses a CENP-C ortholog, but that the bioinformatics lack the resolution to detect it.

Recent information (personal communication from the group of Berend Snel) revealed two CENP-C-like candidates, previously erroneously assigned as MIS18 binding protein (MIS18BP) orthologs. These proteins, that both contain a cryptic CENP-A binding motif, were previously overlooked due to their lack of a carboxy terminal Cupin domain, which is found in most other eukaryotic CENP-C orthologs (E C Tromer, 2017, chapter 3). To verify if these candidates are indeed orthologs of CENP-C, it would be interesting to tag these proteins, with any of the aforementioned tags, to study its localisation and interactors using both immunofluorescence and immunoprecipitation. That way it is possible to identify if this protein is part of the kinetochore and if its localisation and interactions are similar to those of CENP-C orthologs in other eukaryotes. Of note, at the start of this project I tried to amplify these proteins by PCR from a cDNA bank, in order to tag them. However, designing primers for the genes proved to be complicated, because of many repeats and A/T-stretches. An alternative to tagging the entire gene would be to tag only

the CENP-A binding domain of the protein and study its interactions. Additionally, a *Dictyostelium* cell line with CENP-A-GFP exists, which could be used for a GFP pulldown (Dubin et al., 2010). Perhaps CENP-C orthologs would be detected as interactors of CENP-A.

Survivin
The question whether the predicted 'Survivin' gene indeed has the same localisation and function as Survivin in animals/fungi and BORI in plants could not be answered. Only one cell was observed using fluorescence microscopy with a distinct GFP signal that could point to a function in cytokinesis. However, no conclusions can be drawn upon only one observed cell.

In addition to improved mitotic enrichment, generating an antibody against 'Survivin' could aid in the effective detection of this protein. Using an antibody instead of a tag ensures that the tag does not interfere with the native function and localisation of the protein. This is especially relevant for a small protein like Survivin, where most tags are extremely large in comparison to the protein itself. Additionally, it eliminated drawbacks from overexpression, such as slower growth observed in GFP-Survivin overexpressing cells.

Another option would be to perform a pulldown on INCENP-GFP, a cell line which has already been established, to determine the composition of the *Dictyostelium* CPC. Likely, the putative Survivin would show up in this pulldown, as INCENP and Survivin are known interactors in other organisms and this Survivin gene contains the helical domain required to bind to INCENP.

Because the gene does not encode for a phosphate-binding domain, necessary for binding to chromatin, like Survivin and BORI, this protein is possibly only part of the CPC when the complex is on the central spindle during anaphase. This implicate

Conclusion
Concluding, several kinetochore proteins were found in *Dictyostelium discoideum*, but the absence of CENP-C could not be explained. Most likely, comparative genomics methods were insufficient to identify an ortholog of CENP-C, and there are indeed CENP-C-like proteins present in *Dictyostelium*, which will be detected when our methods are optimised.

We could not confirm nor exclude that the helix-only Survivin ortholog indeed functions as Survivin in the CPC. Further research is needed to confirm its localisation and interactions.

Materials & Methods

Genes and primers

A list of all primer sequences can be found in Supplement 2. Primer numbers in the text refer to that list. Primers for all ORFs contain a BamHI restriction site at the N-terminal side and a NheI restriction site at the C-terminal site.

CCAN

Four ORFs (open reading frames) were ordered as genestrings from ThermoFisher/Life Technologies Europe: DdCENP-H, DdCENP-L, DdCENP-S and DdNnf1. The sequences of these genes were predicted using comparative genomics and were adjusted to make them suitable for ordering by changing AT nucleotides to CG where possible without mutating to non-synonymous codons (following ThermoFisher guidelines). A list of substitutions, as well as the exact ordered sequences can be found in Supplement 1. Furthermore, PCR on a cDNA library of mixed life stages (previously made by a former labmember Douwe Veltman) was performed with primers and melting temperatures as noted in the table below, but yielded no cloneable PCR products.

Gene	Primers			Annealing temperature (°C)
Bridgin pt 1	11	+	12	59,5
Bridgin pt 2	13	+	14	60
CENP-O	17	+	18	56,2
CENP-A	19	+	20	61
CENP-K	21	+	22	58
CENP-M	23	+	24	59,5
CENP-N	27	+	28	52
CENP-P	29	+	30	56,2
CENP-C1	31	+	32	52
CENP-C2	33	+	34	55,2
CENP-68	35	+	36	61
Mad1	37	+	38	54,9
Spc24	39	+	40	53,8
CENP-I	41	+	42	53

PCR
For the ordered ORFs, the following primers, melting temperatures and PCR protocol were used:

ORF	Primers	Annealing temperature
CENP-H	15 + 16	52°C
CENP-L	9 + 10	57.5°C
CENP-S	25 + 26	57.5°C
Nnf1	53 + 54	61°C

98°C	30 s	
98°C	10 s	
55°C	20 s	35x
72°C	60 s	
72°C	10 min	

Nnf1 was amplified in a separate PCR with 30 cycles and 5 minutes final extension.

Survivin

The ORF of the hypothetical Survivin gene was ordered at ThermoFisher, of which the sequence can be found in Supplement 1.

PCR
Primers were designed for both C-terminal tagging (1+2) and N-terminal tagging (5+6). PCR was performed with Phusion enzyme (New England Biolabs), with the following protocol:

98°C	30 s	
98°C	10 s	
55°C	20 s	35x
72°C	15 s	
72°C	10 min	

The PCR products were cleaned-up with the Bioké NucleoSpin® Gel and PCR clean-up kit.

Plasmids and cloning

Unless otherwise stated, the concentration of ampicillin in liquid LB and LB agar is 50ug/ml. Plates were poured with 0.1 mg/ml X-gal and 0.5 mM IPTG for blue-white screening. All PCR products were ligated into pBluescript, transformed into *E. coli* DH5α, plated on LB agar with ampicillin, X-gal and IPTG suitable for blue-white screening, and a white colony was picked to grow in LB supplemented with ampicillin. After plasmid isolation, the plasmid was restricted with BamHI-HF and NheI-HF at 37°C overnight, the fragments separated by agarose gel electrophoresis, and the band of the appropriate length was cut out. The Bioké NucleoSpin® Gel and PCR clean-up kit was used to isolate the DNA from the gel. Backbone plasmids (pDK317, pDM1209) were

transformed into *E. coli* DH5α for multiplication and isolated with NucleoSpin® Plasmid EasyPure miniprep kit. This kit was also used in all other plasmid isolations, according to the manual, unless otherwise stated. Unless restriction enzymes could be inactivated by heat, the Gel and PCR clean-up kit was used to get rid of the restriction enzymes every time.

CCAN

TurboID and miniTurbo
The ORFs for TurboID and miniTurbo were ordered from ThermoFisher/Life Technologies Europe with an N-terminal 3xHA-tag and a C-terminal 3xSV40 NLS, and SpeI, NheI and XbaI restriction sites (see Supplement 1). The genestrings were directly ligated into pBluescript and transformed colonies were selected and grown as described under "Plasmids and cloning". The fragments were extracted using SpeI-HF and XbaI restriction enzymes and after agarose gel electrophoresis the band of the appropriate length was cut out and extracted using the Bioké gel extraction kit.

Construction of miniTurbo Gateway vector
Gateway vector pDM627 (hygromycin resistance) was used for the construction of pET17, a miniTurbo vector for episomal expression. pDM627 was restricted with SpeI-HF, and dephosphorylated with FastAP. pDM627 and miniTurbo were ligated with Quick Ligase, and the result was transformed into *E. coli* DB3.1 with 30 min recovery at 37°C. Transformed cells were plated on LB agar supplemented with ampicillin at 37°C overnight. Single colonies were picked and grown in LB with ampicillin at 37°C, 180 rpm overnight. The plasmid was isolated with the miniprep kit, but after lysis and centrifugation, the supernatant was mixed with 96% ethanol before loading it onto the column to maximize the yield (also called Miraprep; Pronobis et al., 2016). The resulting plasmids were checked with ScaI restriction to exclude ligation in the wrong orientation, as well as PCR with D1' primer (43) and miniTurbo forward primer (46). Afterwards, promising candidates were Sanger sequenced with primer 51 (reverse miniTurbo sequencing primer) to verify.

Gateway cloning
The resulting plasmid pET17 contains attR sites to make it suitable for Gateway cloning. This was tried once but yielded no result, so this method will not be described further.

GFP vectors
To tag kinetochore proteins with GFP, the vector pDM1209 was used, which contains a cassette for C-terminal GFP tagging of a protein of interest and G418/neomycin resistance. This vector,

after multiplication in DH5α and subsequent isolation, was restricted in a sequential digest with SpeI and BglII and dephosphorylated with FastAP.

Ligase reaction & transformation
The following genes were ligated with QuickLigase into both pET17 and pDM1209: CENP-H, CENP-L, CENP-S, Nnf1. The ligations were then transformed into DH5α cells with 40 minutes recovery at 37°C after heatshock at 42°C. Afterwards, the cells were grown on LB agar with ampicillin at 25°C for 65 hours. For the miniTurbo vectors, 2 colonies were picked for CENP-H, CENP-L and CENP-S. They were grown in LB with ampicillin at 37°C, 180 rpm overnight. The plasmids were isolated with the miniprep kit and digested with ScaI, followed by agarose gel electrophorese to detect successful ligations. Candidates were then sent for sequencing with primer 51. For the GFP vectors, colony PCR was performed to be able to screen 5 candidates per ligation. In this method, part of a colony is picked and directly put into a PCR mixture, to allow for high throughput screening of colonies. The primers of the genes itself were used, with annealing temperatures: CENP-H 52°C, CENP-L 57.5°C, CENP-S 57.5°C, Nnf1 61°C.

95°C	5 min	
98°C	10 s	
52-61°C	20 s	35x
72°C	60 s	
72°C	5 min	

The products were run in an agarose gel electrophorese. Only the positive candidates were grown in LB with ampicillin at 37°C, 180rpm overnight, followed by plasmid isolation with the miniprep kit. These plasmids were then sent for Sanger sequencing with pDM forward primer and GFP reverse primer (sequences unknown) at Eurofins genomics.

Survivin

Plasmid backbone
To tag the proposed Survivin gene, ligations into several vectors with fluorescent tags were attempted, but only the successful one will be described here. pDK317 was used for an N-terminal GFP-tagging. It was restricted in a sequential digestion with SpeI and BglII, with simultaneous dephosphorylation with FastAP.

Ligase reaction & transformation

Ligation was performed with QuickLigase in QuickLigase buffer for ~20 min. The ligase product was transformed into *E. coli* DH5α, including 30 min recovery at 30°C and plated on LB agar supplemented with ampicillin at 30°C for 42 hours.

Plasmid isolation
Single colonies were picked and grown shaking at 22°C for 4 days in LB supplemented with ampicillin. The plasmid was isolated with the Bioké miniprep kit.

Restriction analysis and sequencing
To check for correct ligation, the isolated plasmids were restricted with ScaI at 37°C overnight, which in case of a correct plasmid gives a characteristic pattern on an agarose gel. One correct candidate plasmid was then sent for Sanger sequencing with primer 43 (D1' reverse) and a GFP forward primer (sequence unknown) at Eurofins Genomics.

Dictyostelium strains and culturing

The following existing *Dictyostelium discoideum* strains were used: AX2 (as negative control and for all transfections except GFP-Survivin), AX3 Aurora-RFP (for GFP-Survivin, from our lab) and AX2 GFP-CENP-68 (provided by Ralph Gräf; Samereier, 2011). Cells were cultured in 9cm Nunc-coated plastic petridishes with HL5 medium supplemented with chloramphenicol (34 ug/mL) at 22°C, unless otherwise stated. Plates were flushed every 2-3 days.

Media and buffers

HL5 Medium including glucose (Formedium)

Peptone	14 g/L
Yeast Extract	7 g/L
Glucose	13.5 g/L
KH_2PO_4	0.5 g/L
Na_2HPO_4	0.5 g/L

Phosphate buffer (PB)
11mM KH_2PO_4
2.75 mM Na_2HPO_4

Phosphate buffered saline (PBS)

137 mM NaCl

2.7 mM KCl

10 mM Na_2HPO_4

1.8 mM KH_2PO_4

Electroporation buffer (EB)

10 mM Na_2HPO_4, pH 6.1

50mM sucrose

Transfections

For every transfection, approximately $2x10^7$ cells were used (approximately one confluent plate). Cells were washed with PB, resuspended in 375 µL EB and mixed with 1-10µL of the DNA (ca. 10µg). The mixture was added to an electroporation cuvette and incubated on ice for 5 minutes. Electroporation was performed with a BTX EMC600 Electroporation System, one pulse of 500V (Capacitance & Resistance mode), 50µE, 13Ω. After another 5 minutes incubation on ice, the cells were added to a plate with 4 µL 0.1M $CaCl_2$ 0.1M $MgCl_2$. After 10 minutes, 8 mL HL5 medium was added with 34 µg/ml chloramphenicol and appropriate selection marker. For hygromycin plasmids, the selection marker was added after 5 hours. After 5-7 days of growth, the medium was replaced with fresh medium as colonies started to form. As soon as the plates were approaching confluency, they were cultured as described above. For each transfection wild type AX2 were used.

Shaking cultures

To initiate shaking cultures, for every strain a full plate was flushed (~1-2x10^7 cells) and added to a 50 ml flask in a total volume of 10 ml HL5 medium. The flasks were shaken at 22°C, 150 rpm overnight. The next day, 10 ml HL5 medium was added. This method prevents the cells from entering a lag phase during the transition from adherent growth to growth in suspension.

Cell cycle synchronisation

For immunofluorescence, cells were seeded at microscope cover slips in a 24-wells plate and placed at 8-10°C for 20 hours in ~1mL HL5 medium. The medium was aspirated and replaced by medium of 22°C, and the cover slips were kept at 22°C for 2 hours to allow the cells to go into mitosis, before fixation.

For pulldown experiments, shaking cultures of 30 ml with densities between $4.5x10^6$ and $1.2x10^7$ were placed in a shaker at 11.5°C, 150 rpm for 22 hours to synchronize the cell cycles. The cells

were pelleted (300g, 3 min) and placed in a new flask with HL5 medium at 22°C. The cultures were shaken at 22°C, 150 rpm for 1:45 hours, after which nocodazole (1:1000 from 2mg/ml 6.7 mM) was added and the cells were shaken for another hour before harvesting. For the biotin pulldown, biotin was added to a concentration of 200 nM (stock: 200µM in DMSO) 2 hours before harvesting. The cells were washed with PB once, snap frozen and stored at -80°C. Samples for IFA were taken before adding the nocodazole, and were fixed 2:50h after removing the cultures from the cold shaker.

Staining and immunochemistry

Primary staining:
α-Tubulin YL1/2 rat (Santa Cruz)

α-CENP-68 serum rabbit (gifted by Ralph Gräf; Samereier, 2011)

α-GFP mouse (Clontech LivingColors JL-8)

α-HA rabbit (Santa Cruz)

Streptavidin-AlexaFluor 488 (Invitrogen)

Secondary/indirect staining:
Goat anti-rat IgG (H&L)-AlexaFluor 647

Donkey anti-rabbit IgG (H&L)-AlexaFluor 568

Goat anti-mouse IgG (H&L)-AlexaFluor 488

Protocol:
Before seeding cells on coverslips, the coverslips were placed in a 24-wells plate, washed with 96% ethanol and dried. Cells were seeded at ~50% confluency and synchronized as described under 'cell cycle synchronisation'. Coverslips with cells were washed once with PB, and then immersed in 4% paraformaldehyde in PB for 10-15 minutes for fixation. They were washed three times with cold PBS including 0.1% Triton X-100 (TX-100). Permeabilization was performed with 0.2% TX-100 in PBS during 10-15 min at room temperature. The coverslips were again washed three times with 0.1% TX-100 in PBS. The cells were then blocked with and kept in 3% BSA in PBS supplemented with 0.02% NaN$_3$ for 1 hour up to a few days at 4°C. The cells were stained with primary antibody (1:1000 dilution in 3% BSA + 0,1% TX-100) for 1 hour at room temperature, washed three times with 0.1% TX-100 in PB or PBS and stained with secondary antibody (1:400 dilution in 3% BSA + 0,1% TX-100) for 1 hour at room temperature. The coverslips were then washed three times with 0,1% TX-100 in PB or PBS. To stain the DNA, the coverslips were covered in DAPI (100ng/mL) for 1-5 minutes and afterwards washed with PB. The coverslips were

then dried by air and mounted on an object glass with ProLong Diamond Antifade Mountant (Invitrogen). Imaging was possible after 18 hours. Cells were imaged with a 63x oil immersion objective with a Zeiss LSM800 Airyscan confocal laser-scanning microscope. Airyscan processing was done using the Zeiss microscope software ZEN.

SDS-PAGE and Western blot

Lysis buffer 2x
100mM Tris/HCL pH 7.5

100mM NaCl

10mM $MgCl_2$

PI-mix 1:100

2% TX-100

10mM DTT

Antibodies
α -GFP mouse (Clontech LivingColors JL-8)

α-mouse HRP m-IgGκ BP-HRP sc-516102 (Santa-Cruz)

Protocol
The cells were pelleted and pellets were frozen in a -80°C freezer. Frozen pellets were resuspended in PB and lysed with lysis buffer. Sample of around $1x10^7$ cells were taken, mixed with 4x SDS loading buffer (0.25 M Tris, 0.28 M SDS, 40% glycerol, 20% 2-mercapto-ethanol, 0.01% w/v bromophenol blue) and boiled for 10 minutes at 95°C. Afterwards they were kept at -20°C. SDS-PAGE was performed on the samples, in a 10-wells (50 µl) Bio-Rad gradient gel. The gel was run at 200V for 35 min, followed by 150V for 10 min. The gel was blotted to a nitrocellulose membrane with Bio-Rad Trans-Blot Turbo at 25V, 2.5 A for 30 min. Blocking was done in 3% BSA in PBS for 1 hour at room temperature. The primary antibody (α-GFP) was diluted 1:1000 in 3% BSA and incubated for 2.5 days at 4°C on a roller. The blot was then washed three times 10 min each time in TBST, followed by incubation with the secondary antibody (α-mouse HRP diluted 1:2500 in 3% BSA) for 1 hour at room temperature. Finally the blot was washed three times 10 minutes in TBST, before imaging with 400uL peroxide solution (Li-Cor WesternSure Premium Stable Peroxide Solution) and 400uL luminol enhancer solution (Li-Cor WesternSure Premium Luminol Enhancer Solution) on a LI-COR Odyssey Fc imager (10 minutes chemiluminescence, 2 minutes 600nm)

Pulldowns/immunoprecipitation

Beads

GFP pulldown: ChromoTek GFP-Trap® Magnetic Agarose

Biotin pulldown: Pierce™ Streptavidin Magnetic Beads

PI mix

Compound	working concentration
Pepstatin	2ug/ml
N-tosyl-l-lysinc chlometyl ketone	100ug/ml
N-p-tosyl-l-arganine-methyl esther hcl	80ug/ml
Leupeptin	5ug/ml
PMSF	0.1 mm
Benzamidine	5 mm

PI tablet: cOmplete™, EDTA-free Protease Inhibitor Cocktail

Buffers GFP pulldown

GFP pulldown lysis buffer (2x)

100mM Tris/HCL pH 7.4

300mM NaCl

PI-mix 1:50 + 1 PI tablet/25mL

1 mM EDTA

1% NP-40 (IGEPAL)

10mM DTT

GFP-pulldown wash buffer

10mM Tris/HCL pH 7.4

150mM NaCl

PI-mix 1:100 + 1 PI tablet/25mL

0.5 mM EDTA

Buffers biotin pulldown

Biotin pulldown lysis buffer (2x)

100mM Tris/HCL pH 7.4

500mM NaCl

PI-mix 1:50 + 1 PI tablet/25mL

0.4%SDS

2mM DTT

4% TX-100

Biotin pulldown wash buffer

10mM Tris/HCL pH 7.4

250mM NaCl

PI-mix 1:50 + 1 PI tablet/25mL

Per assay, around $3x10^8$ cells were taken ($4.41x10^8$ for CENP-H, $4.5 x10^8$ for Nnf1, $3.12 x10^8$ for CENP-68, $2.025x10^8$ for Survivin, $2.40x10^8$ for AX2, $27.15x10^8$ for AX2.b and $3.261x10^8$ for CENP-L), that were synchronized and snap frozen as described under "Dictyostelium strains and culturing". The cells were thawed on ice and lysed in 2x lysis buffer of a volume equal to the cell pellet. The cells were then incubated on ice for 30 minutes, sonicated on a Branson Sonifier 450, 30 pulses, 30% - output level 4 while on ice (CENP-H and Nnf1 were sonicated another 30 pulses after 2 minutes on ice) and pushed through a 25G syringe 10-20 strokes. The lysate was centrifuged for 15 minutes at 4°C. Meanwhile, 200µl beads were taken per assay and washed 3 times with lysis buffer. A sample was taken from the supernatant for SDS-PAGE. The supernatant was loaded onto the beads and the mix was incubated for 2 hours on a rotator at 4°C. The beads were washed one time with 1xlysis buffer, followed by three times with wash buffer. A second sample was taken from the beads in the same volume of wash buffer as the buffer of the first sample. The beads were stored at 4°C before for preparation for mass spectrometry.

SDS-PAGE, Coomassie staining and Western blot

During the pulldown experiment, two samples were taken for each strain: the input sample was taken from the supernatant after centrifugation of the lysate, and the output sample is the beads after pulldown.

SDS-PAGE

The samples were mixed with 4x SDS loading buffer and boiled for 10 minutes at 95°C. An SDS-PAGE was performed on the samples, in two 15-wells (15 µl) Bio-Rad gradient gels. The gels were run at 150V for 60 min.

Coomassie

Coomassie staining was performed on one gel by first washing it 3 times for 5 minutes in demiwater, followed by incubation with Coomassie staining solution (0.02% Coomassie R-250, 30% methanol, 10% acetic acid) on a rocker for 60 minutes. Destaining was performed by washing the gel in demiwater eight times 5-30 minutes, and finally one time for 3 days.

Western blot

The other gel was blotted to a nitrocellulose membrane at 20V for 75 min. The blot was stained with Ponceau stain for 5 min, followed by 5 min washing in demi-water. After imaging, the blot was washed 2 times 5 min in TBST. Blocking was done in 3% BSA in PBS with 0.02% NaN$_3$ for 1 hour at room temperature. The primary antibody (α-GFP) was diluted 1:1000 in 3% BSA with 0.02% NaN$_3$ and incubated for 1 hour at room temperature. The blot was then washed three times 10 min each time in TBST, followed by incubation with the secondary antibody (α-mouse HRP, Santa Cruz) and HRP-streptavidin (Biolegend; both diluted 1:2500 in 3% BSA without NaN$_3$) for 1 hour at room temperature. Finally the blot was washed three times 10 minutes in TBST, before imaging with 400uL peroxide solution (Li-Cor WesternSure) and 400uL luminol enhancer solution (Li-Cor WesternSure) on a LI-COR Odyssey Fc imager (10 minutes chemiluminescence, 2 minutes 600nm)

Bead digestion and protein detection

The protein-bound resins were denatured with 1.6M Urea and reduced with 10mM TCEP for 1h at 37°C. The samples were then alkylated with 10mM iodoacetamide at RT in the dark for 45m and subsequently digested by addition of 1µg sequencing grade modified trypsin at 37°C overnight. After digestion, the supernatants were collected, and the resins were incubated with 1% formic acid for 5 min with agitation. The supernatants were collected and pooled with the previous fractions respectively. The pooled supernatants were cleaned-up by solid phase extraction using C18-tips (Pierce). The cleaned peptides were then subjected to LC-MS analysis using an Ultimate 3000 RSLC nano LC system coupled to a Exploris 480 Mass analyser (Thermo Scientific). The data acquisition was set at data-dependent mode for 60min elution gradient, with full MS mode scanning from 385 to 1540 m/z at a resolution of 120000 for precursor peptide ions. The top 25 precursor ions were selected for fragmentation and MS/MS analysis. The raw data was imported into MaxQuant version 2.1.3.0 (MPI Biochemistry) and analysed against the UniProt *Dictyostelium discoideum* AX4 proteome. The analyses were done mostly with default settings, with the exception of including semi-specific tryptic peptides with a maximum 3 missed-cleavages. Biotinylation on lysine residues and on N-termini (+226.0776) were also included in the related

analyses. Peptide false discovery rate (FDR) was set to 1% using the target-decoy method by default. The protein groups tables were used for statistical analysis.
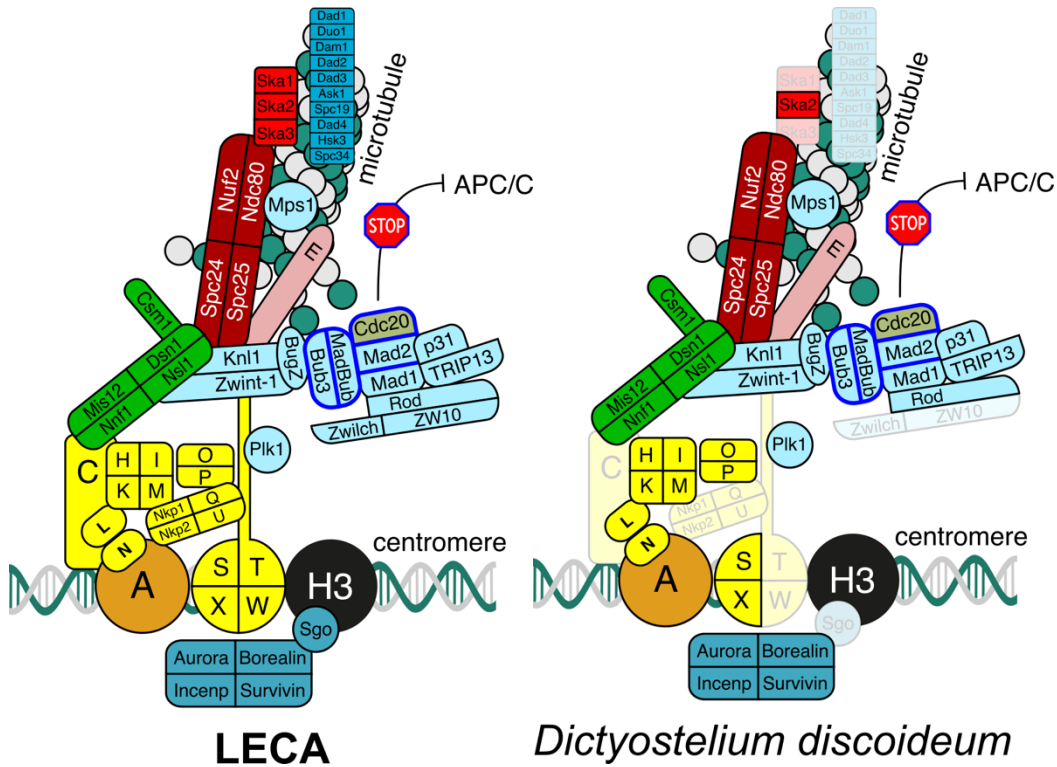
Figures

Figure 1. Eukaryotic kinetochore composition. *A) Reconstructed kinetochore of the Last Eukaryotic Common Ancestor (LECA). The CCAN is shown in yellow, the CPC in dark turquoise. B) The components that are found in Dictyostelium discoideum by means of advanced sequence similarity searches are highlighted.*
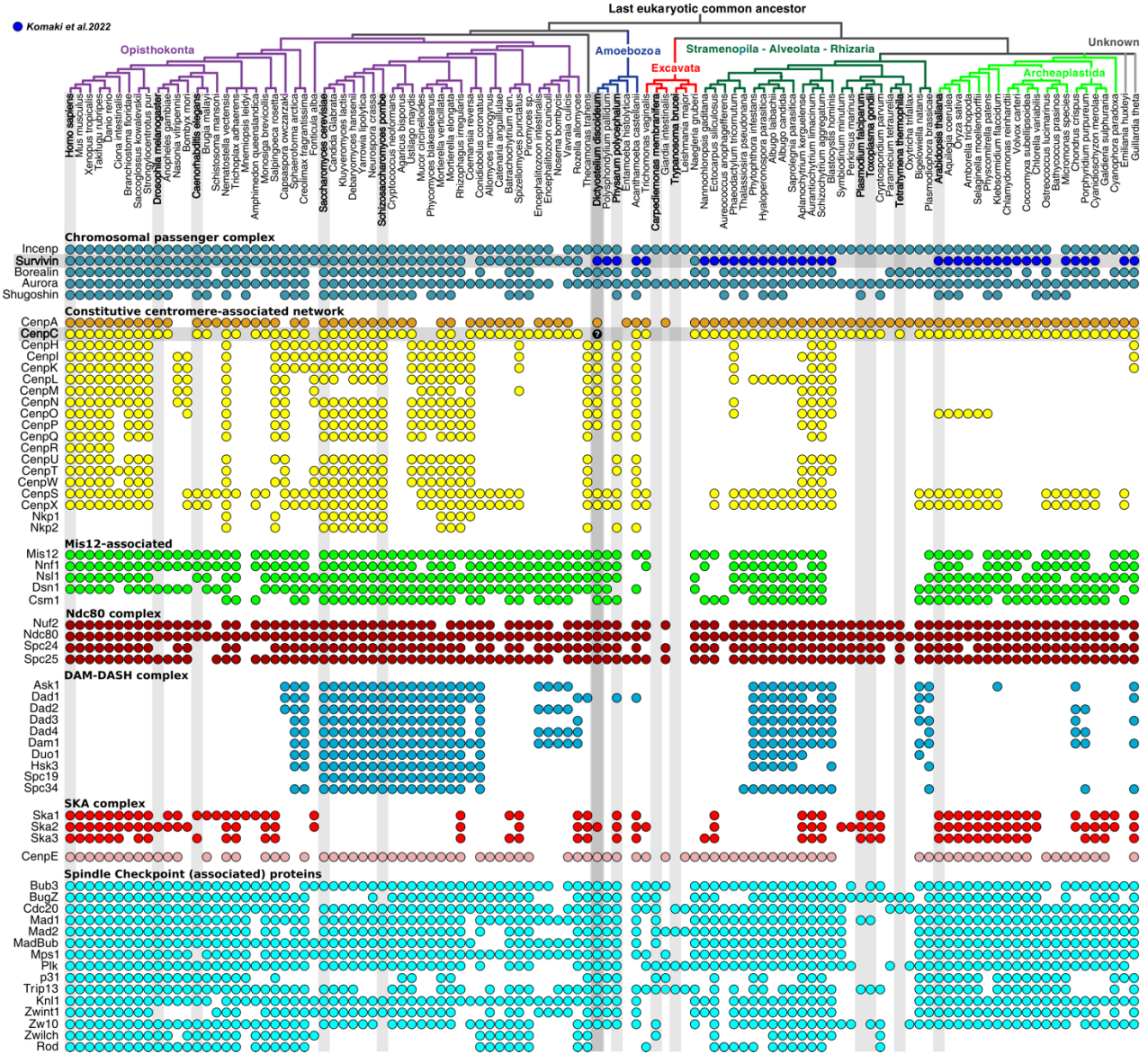*Based on Plowman et al., 2019.*

Figure 2. Presence/absence matrix of kinetochore proteins in a variety of eukaryotic lineages. *Dictyostelium has several CCAN proteins, but is missing CENP-C. A putative Survivin ortholog is found that contains only the C-terminal helix.*
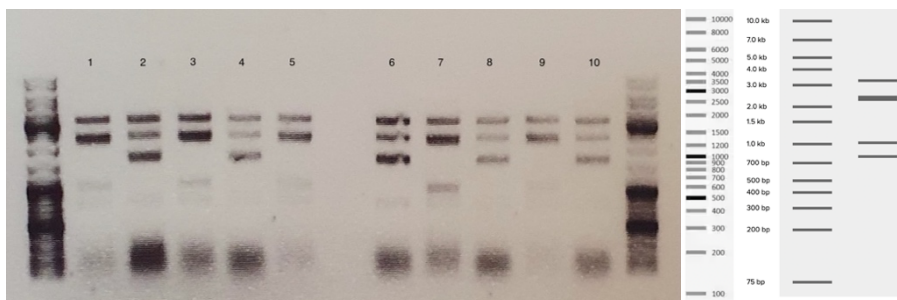
Figure 3. Restriction analysis to check for correct ligation of miniTurbo in pDM627. *A) Ladder, colonies 1-5, empty, colonies 6-10, ladder. Plasmid 1, 3, 5, 7 and 9 show the expected pattern. B) Used ladder: ThermoFisher GeneRuler mix. C) The expected pattern in case of ligation in the correct orientation.*
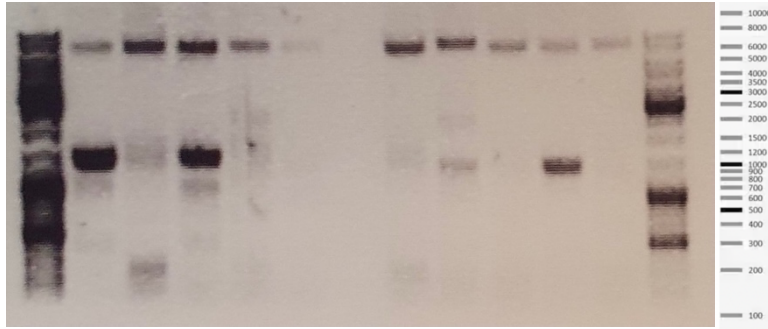
Figure 4. PCR result to check for correct ligation of miniTurbo in pDM627. A) Ladder, colonies 1-5, empty, colonies 6-10, ladder. Colonies 1, 3, 7 and 9 show a band at the expected height. B) Used ladder: ThermoFisher GeneRuler mix.
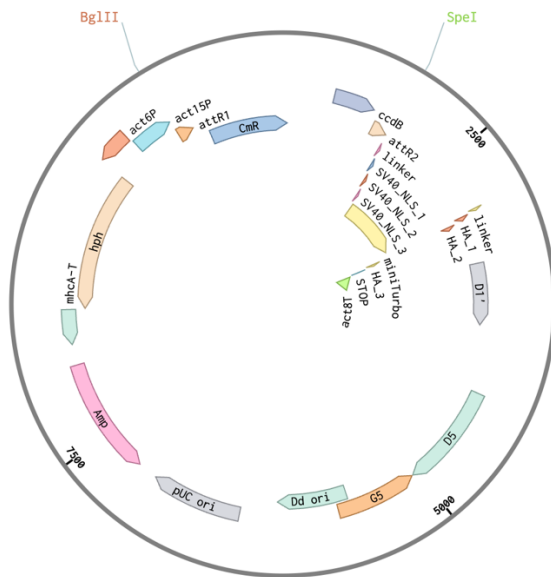
Figure 5. Map of the constructed miniTurbo-vector pET17. In yellow is the miniTurbo gene. On the N-terminal side of the gene is the Gateway cassette. It can be replaced by recombination in a Gateway cloning procedure, or in the conventional way by restriction with BglII and SpeI enzymes. The ccdB gene is toxic for E. coli DH5α.
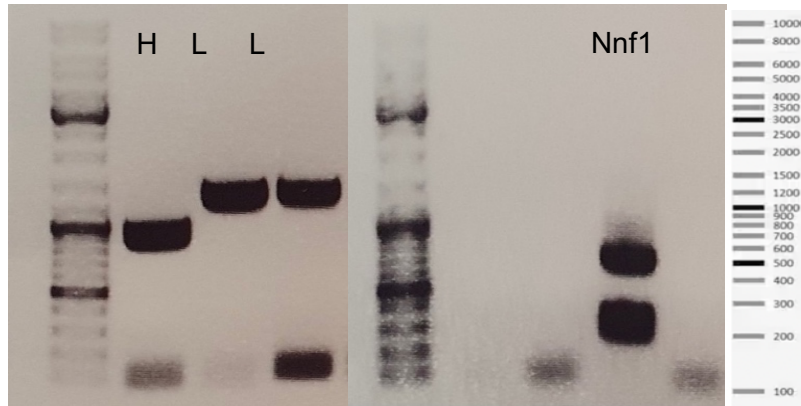
Figure 6. PCR of the ordered ORFs. A) ladder, CENP-H, CENP-L with restriction sites, CENP-L with gateway sequences. B) Nnf1 in the third lane after the ladder. C) Used ladder: ThermoFisher GeneRuler mix.
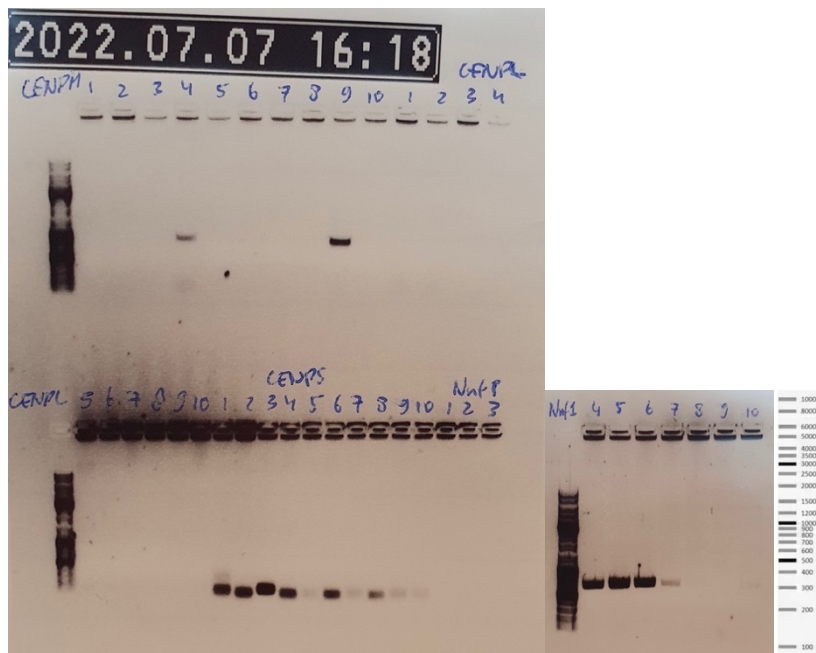
Figure 7. Colony PCR of pDM1209 (GFP vector) ligated with different genes, using primers of the genes. A) and B) CENP-H, CENP-L, CENP-S and Nnf1 each, 10 colonies each. CENPH.4 and Nnf1.4 were chosen after sequencing and used in following experiments. C) Used ladder: ThermoFisher GeneRuler mix.
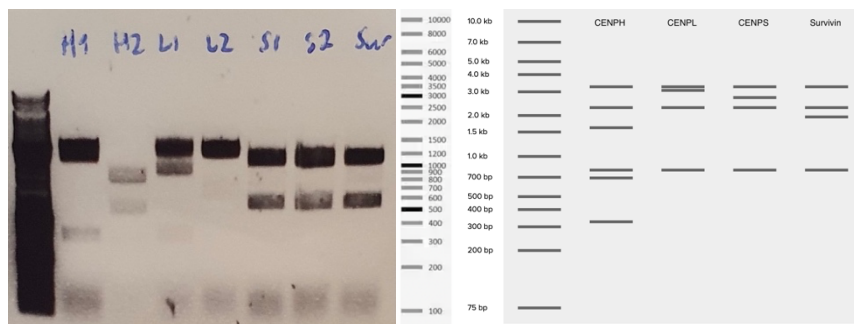
Figure 8. Restriction analysis with ScaI of several ORFs ligated into pET17 (miniTurbo vector). A) Ladder, CENPH (H1 and H2), CENPL (L1 and L2), CENPS (S1 and S2) and Survivin (Sur). B) Used ladder: ThermoFisher GeneRuler mix. C) The expected patterns in case of successful ligation. Only L1 was successful.
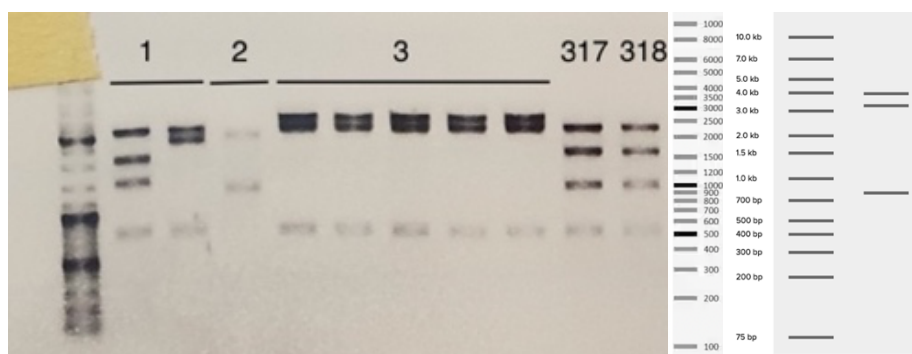

Figure 9. Restriction analysis with ScaI of Survivin ligated into pDK318 (GFP vector). A) The 5 samples marked with 3 are N-terminal GFP (in pDK317), sample marked 317 is pDK317 without insert. B) Used ladder: Thermofisher GeneRuler mix. C) The expected pattern in case of successful ligation.
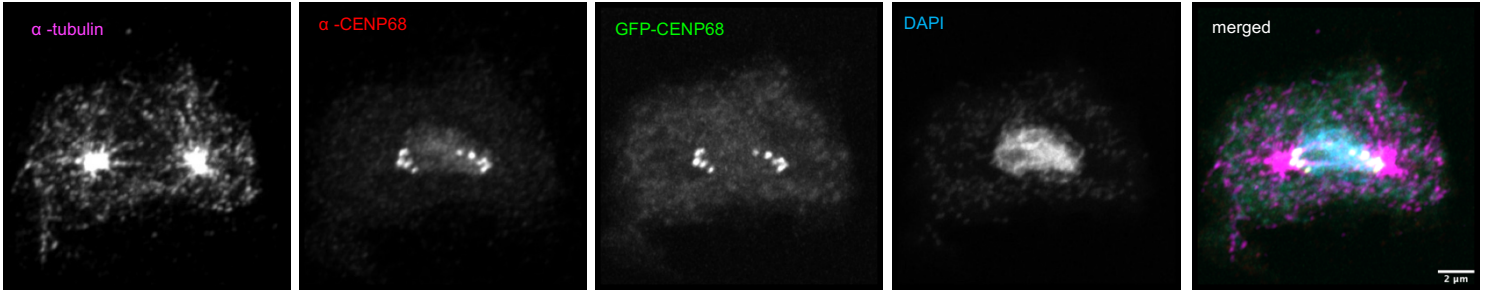
Figure 10. Maximum intensity projection of a cell showing distinct centromeres. *The antibody against CENP-68 and GFP-CENP-68 colocalise, proving both the effectiveness of the antibody and the presence of the tagged CENP68.*
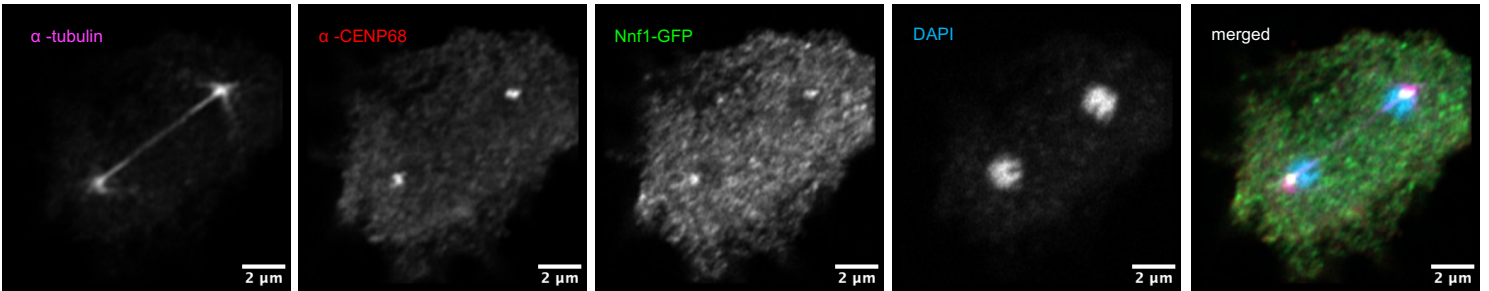

Figure 11. One representative confocal slice of a Nnf1-GFP cell in late anaphase/telophase. *Nnf1-GFP signal can be seen very close to the CENP-68 signal, which corresponds to expected Nnf1 localisation.*
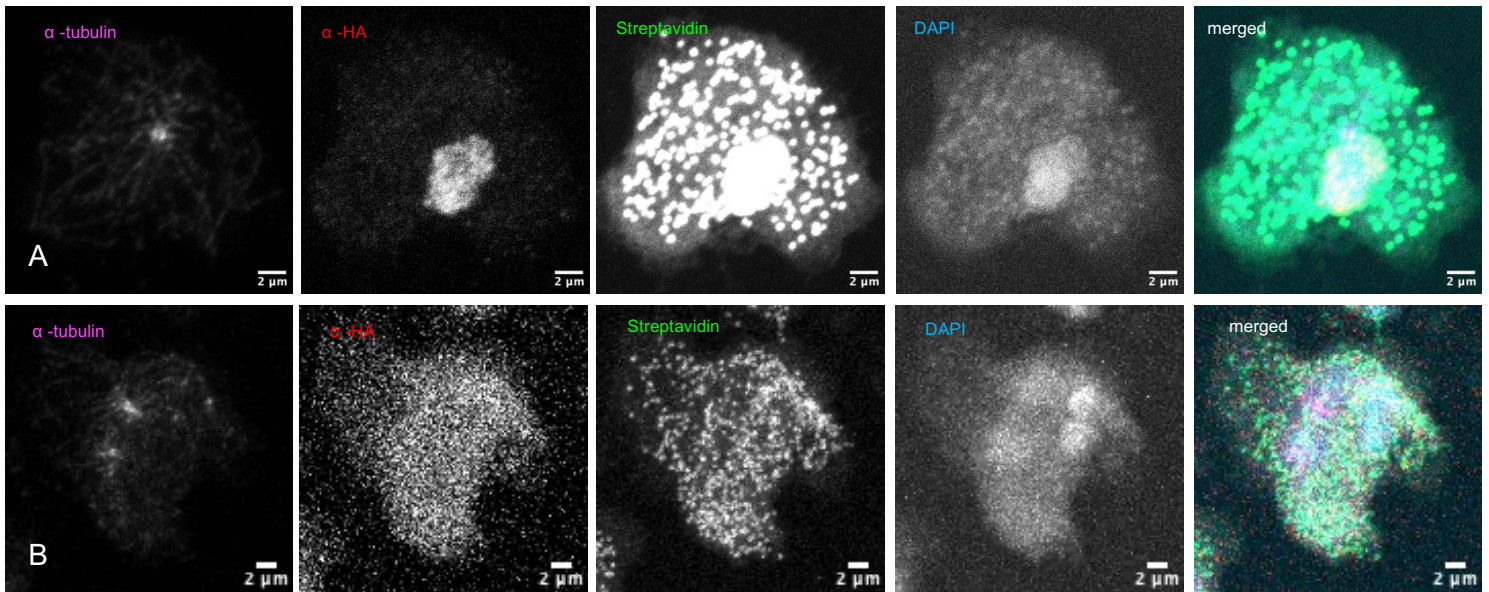

Figure 12. Comparison between a cell expressing CENPL-miniTurbo and an empty AX2 cell. *A: CENP-L-miniTurbo cell, showing both a nuclear HA signal and streptavidin signal. B: negative control AX2 cell, which clearly has no nuclear HA signal or streptavidin signal. In both cells, a polkadot-like pattern is seen, corresponding to mitochondrial morphology.*
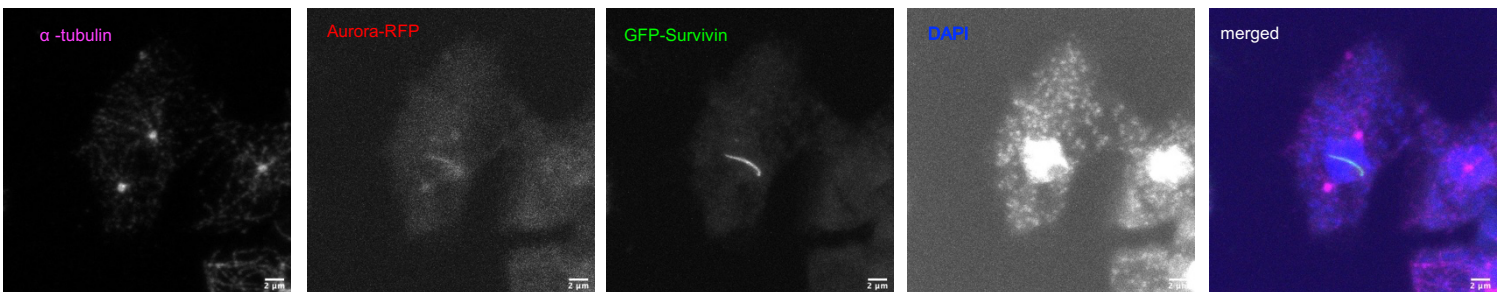

Figure 13. Maximum intensity projection of a cell expressing GFP-Survivin. *GFP-Survivin signal forms a distinct ring-like structure,*
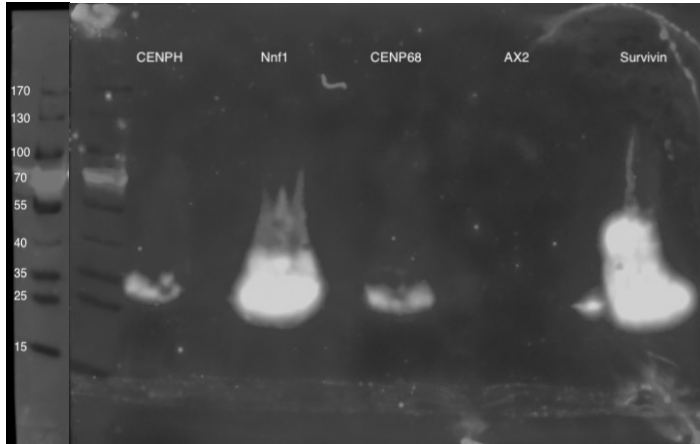
Figure 14. Western blot of unsynchronized GFP-tagged cell lines. CENP-H-GFP, Nnf1-GFP, GFP-CENP-68, AX2 as negative control and GFP-Survivin are indicated.
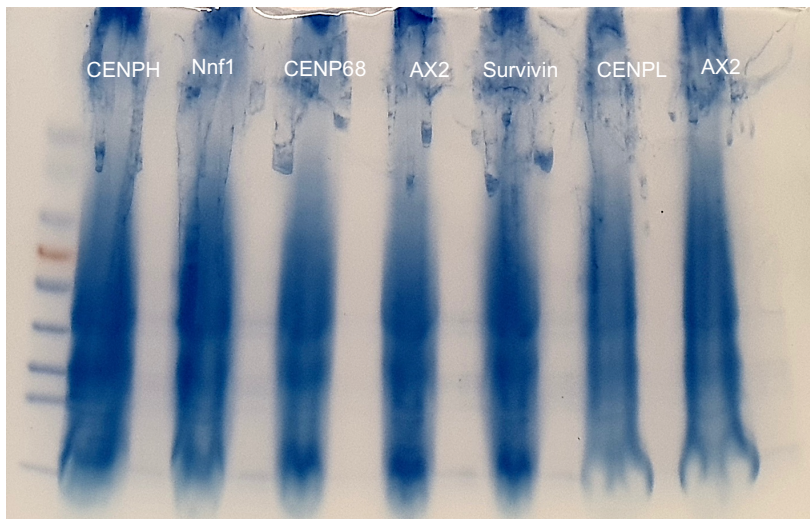

Figure 15. Coomassie stained gel of pulldown samples. Every sample shows the supernatant (input of the pulldown) on the left and sample bound to the beads on the right. CENP-H-GFP, Nnf1-GFP, GFP-CENP-68, AX2 as negative control, GFP-Survivin, CENP-L-miniTurbo, AX2 biotin treated negative control.
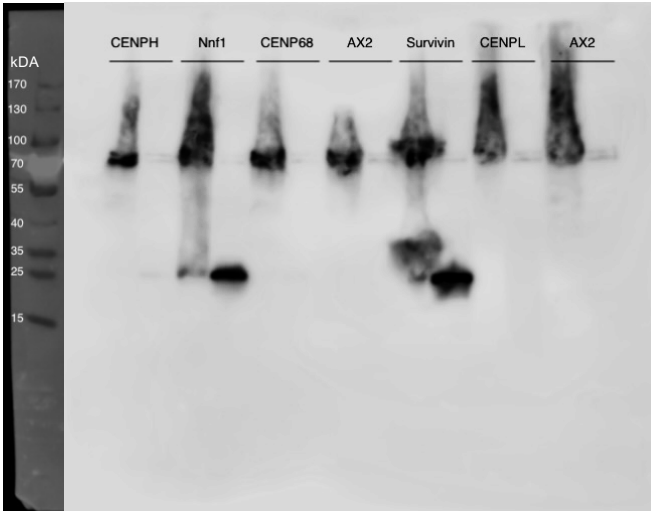
Figure 16. Western blot of the samples taken during the pulldown experiments. *For every cell line is on the left the supernatant after lysis and centrifugation, and on the right a sample of the beads that were sent to the mass spectrometer. From left to right: CENPH-GFP, Nnf1-GFP, GFP-CENP68 (positive control), AX2 (negative control for the GFP pulldown), GFP-Survivin, CENPL-miniTurbo and AX2 (negative control for the biotin pulldown). The blot was stained with anti-GFP with a secondary antibody conjugated to HRP and streptavidin-HRP. The ladder including protein weights is shown on the left.*

UniProt IDs	gene names	complex	aa	enrichment					unique peptides							sequence coverage [%]						
				L	68,0	H	N1	S	AX2-B	L	AX2	68	H	N1	S	AX2-B	L	AX2	68	H	N1	S
Nnf1-GFP	NNF1-GFP (MIS12-C)	MIS12-C	477	0,1	0,1	0,7	22,8	0,1	0	0	0	0	4	37	0	0	0	0	0	27,9	57,7	0
Q54Q64	MIS12 (MIS12-C)	MIS12-C	315	0,7	0,3	0,3	11,1	0,3	0	1	0	0	0	12	0	0	3,2	0	0	0	38,1	0
Q03380	Comitin	actin-related	185	0,5	0,5	0,5	8,0	0,5	0	0	0	0	0	7	0	0	0	0	0	0	48,6	0
Q54DG3	DSN1 (MIS12-C)	MIS12-C	662	0,7	0,7	0,7	4,0	0,7	0	0	0	0	0	3	0	0	0	0	0	0	5,1	0
Q54JS9	actin-binding protein?	actin-related	317	0,4	0,4	2,7	3,6	0,4	0	0	0	0	4	5	0	0	0	0	0	20,5	25,9	0
Q54JG6	TPR_MPL1	nuclear pore	2037	0,9	0,9	0,9	2,0	0,9	0	0	0	0	0	1	0	0	0	0	0	0	0,7	0
Q54K26	ZWINT-1	kinetochore	437	0,9	0,9	0,9	2,0	0,9	0	0	0	0	0	1	0	0	0	0	0	0	2,3	0
Q55DW5	NUP160 (nuclear pore)	nuclear pore	1791	0,9	0,9	0,9	2,0	0,9	0	0	0	0	0	1	0	0	0	0	0	0	0,9	0
Q9U6Y5	GFP	tag	249	0,1	0,5	0,4	2,1	6,3	3	0	0	5	4	18	37	9,3	0	0	14,5	31,2	64,4	70,3
CENPH-GFP	CENPH (HIK-C)	CENP-HIK	546	0,3	0,3	13,0	0,3	0,3	0	0	0	0	12	0	0	0	0	0	0	26,9	0	0
Q55GT6	CENPK (HIK-C)	CENP-HIK	375	0,8	0,8	3,0	0,8	0,8	0	0	0	0	2	0	0	0	0	0	0	8,5	0	0
Q54EX4	CENPI (HIK-C)	CENP-HIK	759	0,8	0,8	3,0	0,8	0,8	0	0	0	0	2	0	0	0	0	0	0	3,4	0	0
Q54QH6	54S ribosomal protein L4	mitochondrion	199	0,5	3,3	2,4	0,5	0,5	0	0	0	4	3	0	0	0	0	0	39,2	28,6	0	0
GFP-Survivin	Survivin	CPC	317	0,3	0,3	0,3	0,3	15,0	0	0	0	0	0	0	14	0	0	0	0	0	0	85,5
P02769	Albumin	human proteiin	607	0,5	0,8	0,3	0,5	6,5	1	1	1	2	0	1	12	2,1	2,1	2,1	4,3	0	2,1	25,4
Q55BV7	MIS18BP	kinetochore	668	6,0	0,5	0,5	0,5	0,5	0	5	0	0	0	0	0	0	7,9	0	0	0	0	0
Q556K7	RING-type domain protein	splicing	723	9,0	0,4	0,4	0,4	0,4	0	8	0	0	0	0	0	0	11,6	0	0	0	0	0
Q55CK7	Zinc finger protein	splicing	544	10,0	0,4	0,4	0,4	0,4	0	9	0	0	0	0	0	0	14,9	0	0	0	0	0
Q54P80	MIF4G	unknown	1395	9,0	0,4	0,1	0,8	0,1	4	26	2	2	0	4	0	3,9	12,7	1,9	2,4	0	4,6	0
Q553S7	Propionyl-CoA carboxylase	BioID background	714	6,7	0,1	0,1	0,1	0,1	47	59	0	0	0	1	0	51,5	55,3	0	0	0	3,1	0
Q8T2J9	Methylcrotonoyl-CoA carboxylase beta	BioID background	588	6,6	0,1	0,1	0,1	0,1	23	31	0	0	0	0	0	42,2	50,9	0	0	0	0	0
Streptavidin	Streptavidin	BioID background	160	5,5	0,1	0,1	0,1	0,1	27	29	0	0	0	0	0	68,8	68,8	0	0	0	0	0
Q54KE6	Methylcrotonoyl-CoA carboxylase alpha	BioID background	699	5,9	0,1	0,1	0,1	0,1	55	59	0	0	0	0	0	66,5	71,4	0	0	0	0	0
Q7KWK7	STU2	kinetchore	1041	3,3	0,8	0,4	1,8	0,4	1	5	0	1	0	3	0	1,5	3,9	0	0,9	0	1,9	0
Q54CA5	DRBM domain protein	mitochondrion	2007	0,7	0,7	3,5	1,8	0,2	0	2	3	2	10	6	0	0	1,4	2,1	1,4	7,7	3,9	0
Q55DJ4	KOW domain protein	mitochondrion	164	0,3	4,4	1,1	1,1	0,3	0	0	1	7	2	2	0	0	0	6,1	43,3	15,2	15,2	0
Q54F42	NADH dehydrogenase alpha	mitochondrion	124	0,6	0,6	3,4	0,6	0,6	0	0	1	0	3	0	0	0	0	12,1	0	37,1	0	0
Q8T673;Q8T675	ABC transporter G family member 21	ABC transporter	1449	1,3	3,4	0,6	0,6	0,6	0	1	0	3	0	0	0	0	3,6	0	3,9	3,1	3,7	0
Q86AD5	Pyruvate dehydrogenase	metabolism	413	0,3	2,8	2,5	0,6	0,1	0	1	8	13	12	3	0	0	5,6	26,4	29,3	38	7,3	0
Q54TY5	ABC transporter G family member 21	ABC transporter	182	0,5	3,8	0,5	0,5	0,5	0	0	2	4	0	0	0	0	0	12,6	33	0	0	0

Figure 17. Selection of proteins detected by mass spectrometry in GFP- and biotin pulldowns. AX2 cells treated with biotin (AX2-B) as negateive control for the biotin pulldown, CENP-L-miniTurbo (L), AX2 cells as negative control for GFP pulldown (AX2), GFP-CENP-68 (68), CENP-H-GFP (H), Nnf1-GFP (N1), GFP-Survivin (S).

Bibliography

Akhmanova, A., & Hoogenraad, C. C. (2005). Microtubule plus-end-tracking proteins: mechanisms and functions. *Current Opinion in Cell Biology*, *17*(1), 47–54. https://doi.org/10.1016/j.ceb.2004.11.001

Batsios, P., Gräf, R., Koonce, M., Larochelle, D., & Meyer, I. (2019). Nuclear envelope organization in Dictyostelium discoideum. *The International Journal of Developmental Biology*, *63*, 509–519. https://doi.org/10.1387/ijdb.190184rg

Bozzaro, S. (2013). *The Model Organism Dictyostelium discoideum BT - Dictyostelium discoideum Protocols* (L. Eichinger & F. Rivero (eds.); pp. 17–37). Humana Press. https://doi.org/10.1007/978-1-62703-302-2_2

Branon, T. C., Bosch, J. A., Sanchez, A. D., Udeshi, N. D., Svinkina, T., Carr, S. A., Feldman, J. L., Perrimon, N., & Ting, A. Y. (2018). Efficient proximity labeling in living cells and organisms with TurboID. *Nature Biotechnology*, *36*(9), 880. https://doi.org/10.1038/NBT.4201

Brusini, L., Dos Santos Pacheco, N., Tromer, E. C., Soldati-Favre, D., & Brochet, M. (2022). Composition and organization of kinetochores show plasticity in apicomplexan chromosome segregation. *The Journal of Cell Biology*, *221*(9). https://doi.org/10.1083/jcb.202111084

Cheeseman, I. M., Chappie, J. S., Wilson-Kubalek, E. M., & Desai, A. (2006). The Conserved KMN Network Constitutes the Core Microtubule-Binding Site of the Kinetochore. *Cell*, *127*(5), 983–997. https://doi.org/10.1016/j.cell.2006.09.039

Chia, C. P., Inoguchi, N., Varon, K. C., Bartholomai, B. M., & Moriyama, H. (2020). Mitochondrial localization of Dictyostelium discoideum dUTPase mediated by its N-terminus. *BMC Research Notes*, *13*(1), 16. https://doi.org/10.1186/s13104-019-4879-7

Desai, A., Rybina, S., Müller-Reichert, T., Shevchenko, A., Shevchenko, A., Hyman, A., & Oegema, K. (2003). KNL-1 directs assembly of the microtubule-binding interface of the kinetochore in C. elegans. *Genes & Development*, *17*(19), 2421–2435. https://doi.org/10.1101/gad.1126303

Dubin, M., Fuchs, J., Gräf, R., Schubert, I., & Nellen, W. (2010). Dynamics of a novel centromeric histone variant CenH3 reveals the evolutionary ancestral timing of centromere biogenesis.

Nucleic Acids Research, *38*(21), 7526. https://doi.org/10.1093/NAR/GKQ664

Hinshaw, S. M., & Harrison, S. C. (2019). The structure of the Ctf19c/CCAN from budding yeast. *ELife*, *8*, e44239. https://doi.org/10.7554/eLife.44239

Kelly, A. E., Ghenoiu, C., Xue, J. Z., Zierhut, C., Kimura, H., & Funabiki, H. (2010). Survivin Reads Phosphorylated Histone H3 Threonine 3 to Activate the Mitotic Kinase Aurora B. *Science*, *330*(6001), 235–239. https://doi.org/10.1126/science.1189505

Kim, D. I., Birendra, K. C., Zhu, W., Motamedchaboki, K., Doye, V., & Roux, K. J. (2014). Probing nuclear pore complex architecture with proximity-dependent biotinylation. *Proceedings of the National Academy of Sciences of the United States of America*, *111*(24), E2453-61. https://doi.org/10.1073/pnas.1406459111

Kline, S. L., Cheeseman, I. M., Hori, T., Fukagawa, T., & Desai, A. (2006). The human Mis12 complex is required for kinetochore assembly and proper chromosome segregation. *The Journal of Cell Biology*, *173*(1), 9–17. https://doi.org/10.1083/jcb.200509158

Komaki, S., Takeuchi, H., Hamamura, Y., Heese, M., Hashimoto, T., & Schnittger, A. (2020). Functional Analysis of the Plant Chromosomal Passenger Complex. *Plant Physiology*, *183*(4), 1586–1599. https://doi.org/10.1104/pp.20.00344

Komaki, S., Tromer, E. C., De Jaeger, G., De Winne, N., Heese, M., & Schnittger, A. (2022). Molecular convergence by differential domain acquisition is a hallmark of chromosomal passenger complex evolution. *Proceedings of the National Academy of Sciences of the United States of America*, *119*(42), e2200108119. https://doi.org/10.1073/pnas.2200108119

Kops, G. J. P. L., Weaver, B. A. A., & Cleveland, D. W. (2005). On the road to cancer: aneuploidy and the mitotic checkpoint. *Nature Reviews Cancer*, *5*(10), 773–785. https://doi.org/10.1038/nrc1714

Luo, Q., Michaelis, C., & Weeks, G. (1994). Overexpression of a truncated cyclin B gene arrests Dictyostelium cell division during mitosis. *Journal of Cell Science*, *107 (Pt 1*, 3105–3114. https://doi.org/10.1242/jcs.107.11.3105

Maeda, Y. (1986). A new method for inducing synchronous growth of Dictyostelium discoideum cells using temperature shifts. *Journal of General Microbiology*, *132*(5), 1189–1196.

https://doi.org/10.1099/00221287-132-5-1189

Pears, C. J., & Gross, J. D. (2021). Microbe Profile: Dictyostelium discoideum: model system for development, chemotaxis and biomedical research. *Microbiology (Reading, England)*, *167*(3). https://doi.org/10.1099/mic.0.001040

Pesenti, M. E., Raisch, T., Conti, D., Walstein, K., Hoffmann, I., Vogt, D., Prumbaum, D., Vetter, I. R., Raunser, S., & Musacchio, A. (2022). Structure of the human inner kinetochore CCAN complex and its significance for human centromere organization. *Molecular Cell*, *82*(11), 2113-2131.e8. https://doi.org/10.1016/j.molcel.2022.04.027

Petrovic, A., Keller, J., Liu, Y., Overlack, K., John, J., Dimitrova, Y. N., Jenni, S., van Gerwen, S., Stege, P., Wohlgemuth, S., Rombaut, P., Herzog, F., Harrison, S. C., Vetter, I. R., & Musacchio, A. (2016). Structure of the MIS12 Complex and Molecular Basis of Its Interaction with CENP-C at Human Kinetochores. *Cell*, *167*(4), 1028-1040.e15. https://doi.org/10.1016/j.cell.2016.10.005

Plowman, R., Singh, N., Tromer, E. C., Payan, A., Duro, E., Spanos, C., Rappsilber, J., Snel, B., Kops, G. J. P. L., Corbett, K. D., & Marston, A. L. (2019). The molecular basis of monopolin recruitment to the kinetochore. *Chromosoma*, *128*(3), 331–354. https://doi.org/10.1007/s00412-019-00700-0

Pronobis, M. I., Deuitch, N., & Peifer, M. (2016). The Miraprep: A Protocol that Uses a Miniprep Kit and Provides Maxiprep Yields. *PloS One*, *11*(8). https://doi.org/10.1371/JOURNAL.PONE.0160509

Salas-Leiva, D. E., Tromer, E. C., Curtis, B. A., Jerlström-Hultqvist, J., Kolisko, M., Yi, Z., Salas-Leiva, J. S., Gallot-Lavallée, L., Williams, S. K., Kops, G. J. P. L., Archibald, J. M., Simpson, A. G. B., & Roger, A. J. (2021). Genomic analysis finds no evidence of canonical eukaryotic DNA processing complexes in a free-living protist. *Nature Communications*, *12*(1), 6003. https://doi.org/10.1038/s41467-021-26077-2

Samereier, M. (2011). *Functional analyses of microtubule and centrosome-associated proteins in Dictyostelium discoideum* [University of Potsdam]. http://nbn-resolving.de/urn:nbn:de:kobv:517-opus-52835

Schauer, T. M., Nesper, M., Kehl, M., Lottspeich, F., Müller-Taubenberger, A., Gerisch, G., &

Baumeister, W. (1993). Proteasomes from Dictyostelium discoideum: Characterization of Structure and Function. *Journal of Structural Biology*, *111*(2), 135–147. https://doi.org/https://doi.org/10.1006/jsbi.1993.1044

Schulz, I., Erle, A., Gräf, R., Krüger, A., Lohmeier, H., Putzler, S., Samereier, M., & Weidenthaler, S. (2009). Identification and cell cycle-dependent localization of nine novel, genuine centrosomal components in Dictyostelium discoideum. *Cell Motility and the Cytoskeleton*, *66*(11), 915–928. https://doi.org/10.1002/cm.20384

Tian, T., Chen, L., Dou, Z., Yang, Z., Gao, X., Yuan, X., Wang, C., Liu, R., Shen, Z., Gui, P., Teng, M., Meng, X., Hill, D. L., Li, L., Zhang, X., Liu, X., Sun, L., Zang, J., & Yao, X. (2022). Structural insights into human CCAN complex assembled onto DNA. *Cell Discovery*, *8*(1), 90. https://doi.org/10.1038/s41421-022-00439-6

Tromer, E C. (2017). *Evolution of the Kinetochore Network in Eukaryotes*. Utrecht University.

Tromer, Eelco C, van Hooff, J. J. E., Kops, G. J. P. L., & Snel, B. (2019). Mosaic origin of the eukaryotic kinetochore. *Proceedings of the National Academy of Sciences, 116*(26), 12873–12882. https://doi.org/10.1073/pnas.1821945116

Varma, D., & Salmon, E. D. (2012). The KMN protein network – chief conductors of the kinetochore orchestra. *Journal of Cell Science*, *125*(24), 5927–5936. https://doi.org/10.1242/jcs.093724

Warren, C. D., Brady, D. M., Johnston, R. C., Hanna, J. S., Hardwick, K. G., & Spencer, F. A. (2002). Distinct Chromosome Segregation Roles for Spindle Checkpoint Proteins. *Molecular Biology of the Cell*, *13*(9), 3029–3041. https://doi.org/10.1091/mbc.e02-04-0203

Weiner, O. H., Murphy, J., Griffiths, G., Schleicher, M., & Noegel, A. A. (1993). The actin-binding protein comitin (p24) is a component of the Golgi apparatus. *The Journal of Cell Biology*, *123*(1), 23–34. https://doi.org/10.1083/JCB.123.1.23

Welker, D. L., & Williams, K. L. (1980). Mitotic arrest and chromosome doubling using thiabendazole, cambendazole, nocodazole and ben late in the slime mould, Dictyostelium discoideum. *Journal of General Microbiology*, *116*(2), 397–407. https://doi.org/10.1099/00221287-116-2-397/CITE/REFWORKS

Xiao, H., Verdier-Pinard, P., Fernandez-Fuentes, N., Burd, B., Angeletti, R., Fiser, A., Horwitz, S. B., & Orr, G. A. (2006). Insights into the mechanism of microtubule stabilization by Taxol. *Proceedings of the National Academy of Sciences*, *103*(27), 10166–10173. https://doi.org/10.1073/pnas.0603704103

Yamashita, K., Iriki, H., Kamimura, Y., & Muramoto, T. (2021). CRISPR Toolbox for Genome Editing in Dictyostelium . In *Frontiers in Cell and Developmental Biology* (Vol. 9). https://www.frontiersin.org/articles/10.3389/fcell.2021.721630

Yan, K., Yang, J., Zhang, Z., McLaughlin, S. H., Chang, L., Fasci, D., Ehrenhofer-Murray, A. E., Heck, A. J. R., & Barford, D. (2019). Structure of the inner kinetochore CCAN complex assembled onto a centromeric nucleosome. *Nature*, *574*(7777), 278–282. https://doi.org/10.1038/s41586-019-1609-1

Yatskevich, S., Muir, K. W., Bellini, D., Zhang, Z., Yang, J., Tischer, T., Predin, M., Dendooven, T., McLaughlin, S. H., & Barford, D. (2022). Structure of the human inner kinetochore bound to a centromeric CENP-A nucleosome. *Science*, *376*(6595), 844–852. https://doi.org/10.1126/science.abn3810

Zhu, H. (2012). Protocol to Determine Mitotic Index by FACS. *Bio-Protocol*, *2*(6), e196. https://doi.org/10.21769/BioProtoc.196

Acknowledgements

Supplementary material

Supplement 1: Genes

CENP-H

Ordered gene:

ATGAATCATAACGAAGAAGATATAAAGAATATCAAAATTACCTCAAAGAGAATATTAAAAACAGTACTAAATGCAAAAGTAGGTGC
AAATAAGATTCAACTCAAAAGGGGAATAACAGAGTTATCAAGAGGCACTGAATCAATTTTAAATTTAGAGAATCAAAAACTCTCAA
TTTTAGGTCAATTACAAATTGAATCAAAAAAACTAAAATACCTAAAATCTGCTAATAATCAAGAAGAAATAGAAGCAGAAGTAGAA
GAACAGGAAGAAGTAGAAGAAGAAGAGGAATTATATGAAGAAGTAGAAGTAGAGTCAGAGCAAATCAAGGTTGATTATGATAAA
GATGAAAATTATGAAAATGAACTAAAGAGAATTGATGATATAAATGATGAATTAAGACTTCAAGTTTTACAATTATCTGAAATAAAA

TCAGAACAACAATTAACTTTCAATAGAATAATTCAAAGTGAAGTAATTAATTTTATATCCAATCAAGAACTATTTGAAGATAATGAA
AATGAAAAACTATTTCAATTGATTAAATGTAGAGATAGATTGGTTTTAAGGTGTTTAGAACTAATTTCACAAATTAAAAGAACAGAT
ATTAATATTTTCAACATAGAAAGGAAAAGAAATGATCAATTCGTTGAAAATAGATTTTTAGCTGATTATTATTTTGATACATGTGGT
GGTGGTGGTTCAAGAGTATTAGGTGGAAATGAATTCCAGTATTTAAAAAATGTGGAAGAAAGTACTGCAAAAATAATAGAGGCTT
TAATTTATAGATCAAAGATTAATTGGTGTTATAATGAAAATTTCAAGAAATTCTTTAACAAAAAATACGACTCTGAAAAAAATAAAG
AACAAACATTCATATTACTTCAGGGAAATAAAAATAAAAAATAG

Changes to predicted ORF:
C21T, T67C, A156G, T205C, T213C, T214C, A285G, A312G, T364C, A489, T526C, T615C,
T618C, A792G, T819C, A822G, A906G.

CENP-L

Ordered gene:
ATGGAAAATGATATTTTAAAAGATTTAGATATATATCTTCAAAAAGAATGTGAAAAATTTAAATCATTTGATTCATTTAAAAATGTTC
CTTGGAATATTCATAGAGTAACTCCACTTTTTAATTTTAAAATACAAAAATATGGTAATGATATAATGTTACAAAGAAATTATTTGAA
TAAATTAACAAGTGATTTAAATCAATTTTTATCTCATAATTTAGCATCAATAAAAAGAAATCGTCATTTTGCCTATGAATGTAAAATT
TTAATAATAGAACTTGATCCAAATATAATCAAAGAAATGAATTATTTCCAAGTATTGGTATTTATATTTCTTCAAAAAATATAGAAG
CAAATGTAAATAAATTTTCAAAAATAGTATTGGTTTCATGTAGAAATATTGATACAGAAAAAGGAACTTCATGTAAAAATAATTCTA
GTGAGCCGCAACTTCTTTCATATAATATGGTACTTTCAAATGGTGATAAAGAAATAATAAAGGAAGCCACAAAATGGTTGCATTTT
AAATATGATTGCTCCATTTCCGATGTTATAATTCAACCTTCATATATTTATTCATTAATGTTACTTTGGATGACTAGAAATTCTGATA
AATTTTTTAATAGATTAACAACATCAACAGAAACAAAAAATACAACACCAAAGAAAATAATTAATGATGAAAAACATAAAAAAATTC
GATATATCGATCAAGAGTATGATATTGATGATTATGAGCATTATGCTAATCAAGAAGATGACGAAGATGACGAGGAGAAAGAAGA
AAAAGGAGAGGAAGAAGAGGAGGAAGAAACTGATAAAGAAGAAGAAATAGATAAGGAAGAGAATTTATCAAACATTGAAGTTTC
TGAAGATAAGTGTTCAGATGATGAGGAAGATGAAGAAGATAAAGAACTAAATAATAAAAACGATCAAAAAGAAAGAGAGAAAAT
ACATCAAAAATCTCAATGAAACAATTCGAATTTATATATTCTTTTGGTCCTACTATGGGCAGAATTAAAAAAAAAGAAGAAAATGAT
CAATCATTACAACTTCTTACTTTAAAAGTTCCTTCAAAAACAATGTATAGAATAATTTCACATTGCAATAATGTCAATCCAAAATTTA
ATTCGCTTGAAAAAAGTTTAAAAGCAAATCAAATAATGGAAATTTTGGGTAATAATTTTAAAAAAATTTTAGGTTTTTCTTTAGATTC
TTTAGCATTTGTTCGAGTTGTAACATCTGAAGCATCACTGGAAGTTTCTGGAAAAGTTAATATTTTTAGAGATCCTTTTATTACTTT
AACAGATTTATCAACATATGTTTAA

Changes to predicted ORF:
T132A, A174G, A208T, G209C, T762C, T771C, A774G, A777G, G798A, A804G, A807G,
T834A, A1176G, C1290T.

CENP-S

Ordered gene:
ATGTCAGATATCGATGATTTTGAGTCAGATGGTGAGGGTGGAAAAATTTACAAGAAGTTCGTCATCGACCACAAGAAGCGGAAG
CAGCACCAGCTGAAAACAAAGCTGATCAACAACAATAGCAGCAGCCTGAAGGCCAAGCAGCTGAAGTCCACCATCACCACCAC
CACAACTACCACCAGCAAGAAGAAGCAGCGGCCCATCATCAGCCTGGAAAGCGACTCCGACGAGACAGAGGACGAGATCGGC
TACATCAAGAAGAAAACGACCACGACCACACTGAAGCCTAAGTACCCTACCACAACCACCTCCACCAGCACAAGCACCAGCAA
CAGACCCAAGAACGACCTGATCTTCGACGACGAGGTGGACGAGGATAATAACAATAATAACAATCTGGACGAGGACAGGCCCA
TCTTCAAGCCCAACAAGAAAAAGCGGGCCAGCATCAACGATGAGATCGAGAACGACGACAATGATGAGGACAACAGCACCGTG
TCCAACTACGACAAGTACAAGACCTTCGACGAGCTGGATGGCAACGACAAGTTCAACAACAACAATAACTCCAACAAGCCCACC
AAGAAGAAAACCACAACAACCACCACCACGACCAACAAGATCGACAAGTTCGACTCCAACACCATCGACAAGATCAAGCAGAG
CCTGCACTACAGCGTGATCAAGGTGTCCGAGGAACAGGCCAACAAGTTTAACGTGGGCATCACCAAAGAAACCATGAGCAGCC

TGTCCGAGCTGATCTTCAACGTGACCAAGGACCTGGTGTCCAAAGATCTGGTGTCTTTCGCCCAGCACGCCAAGCGGCCTACC
AAGATCACAGTGGACGACGTGAAGCTGCTGGCCAGAAGAAACGACAGCCTGCTGAACTCCCTGCTGCTGAAAGAAACCGAGA
GAGAGCGCGAGCTGGAACTGCAAGAGGTGGTCAACAAGTCCTCTAAGAAGAAGGACAACAACAATAACATCATCCAGTTCGAC
GACTGA

Changes to predicted ORF:
C444T, C450T, C453T, C627T, C1041T, Δ109-183

Nnf1

Ordered gene:
ATGAACAACAACAACTCCAACAACAACAATAACAATAATAACAACAACAACGACAAAACAAGTAATAATACAATAGAAAAAACCAC
AACACTAAATGTAGATTATGATAAAGGTATATTAAATTTGGAAATTGGTGAGAGTGACATTTTAAAATGTATTTCAGGAGAGATAG
AAGGAATTAGAATGATAAAATTAAGAATGTTTCACGATTTAGTAATAGATAAATCATTATCAGAATTACCGTTTCAGAAATTCTATG
ATTGTTACTCATCTTTAAATAATAACAACTTGAATACAAAATCATTTTTATCTTATCTTTATACAAATGTATTTCAAACTTTATCAGAA
AGAATAAAGAGTGATTTTCAATTAATATGTCAAGAAAGACAAATTTCAATTAGATTAAGTGAATTAGAAAGATTACTTCGTGAACA
ACCAACCATTCTCAACGATAAAAGAGCACCTCCATCAAGTATAATTAATCCTGAAGAACAAATAATGTCACAAATCATAGATTTAA
AGATGACTGAAAGGGAAAGATTATTAAAAATCTATCAGAATCTATTAAATGAAAATAAGAAGATAAAAAGACAAGAAACAGATTTA
GAGAAACAAAAAACAGTTTTAGTTGACCAAATTAATACAAAAATAGAGAATATTAAGAAAATAGTTGATCTTTCTGTGTCACTCGA
TTCATAA

Changes to predicted ORF:
None

Survivin

ATGGATAAAAAAGATCAATTATATAAACAAATGTCAATGGATAGTAATAGTGGATTAAATTTTGAACAATTAAAGAAATTAAAAGTG
GAAGAGTATATAGAGTTTCAATATAATCGTCAAATTGAACTTTTAAATAAATATACAGAAAATAAAATCCAAGAAATTGTAAATCAC
AAAGAAAAATTAAAAAGAGAATTAATTGAACAACAAAGAAATCAAGAAAATTAA

TurboID

Ordered gene:
ACTAGTGGTGGAAGTGGTGGATCTCCAAAGAAGAAGCGTAAGGTAGATCCAAAGAAGAAGAGAAAAGTTGATCCAAAGAAAAAA
AGGAAGGTTGCTAGCAAAGATAATACTGTTCCATTGAAATTAATAGCATTATTAGCAAATGGTGAATTTCATTCTGGTGAGCAATT
AGGAGAAACTTTAGGTATGTCAAGAGCTGCAATTAATAAGCATATACAAACTTTACGTGATTGGGGTGTAGATGTATTCACTGTT
CCAGGTAAAGGTTATTCATTACCAGAACCAATACCATTATTAAATGCTAAACAAATATTAGGACAATTAGATGGAGGTTCAGTAG
CAGTATTACCAGTAGTTGATTCAACAAATCAATATTTATTAGATCGTATTGGAGAATTAAAGAGTGGTGATGCATGTATTGCTGAG
TACCAACAAGCTGGTAGAGGTTCTCGTGGTCGTAAATGGTTTAGTCCATTTGGTGCTAATTTATATTTATCCATGTTCTGGAGATT
AAAGAGAGGTCCAGCTGCAATAGGATTAGGTCCAGTAATTGGAATTGTAATGGCTGAAGCATTACGTAAATTAGGTGCAGATAA
GGTAAGAGTTAAATGGCCAAATGATTTATATTTACAAGATAGAAAGTTAGCTGGAATATTAGTTGAGTTAGCTGGTATAACTGGT
GATGCTGCACAAATTGTTATAGGTGCTGGAATAAATGTTGCTATGAGACGTGTAGAGGAAAGTGTTGTAAATCAAGGATGGATA
ACTTTACAAGAAGCAGGTATAAATTTAGATAGAAATACTTTAGCAGCTACTTTAATACGTGAGTTAAGAGCAGCTTTAGAATTATT
CGAGCAAGAAGGTTTAGCACCATATTTACCAAGATGGGAGAAGTTAGATAATTTCATAAATCGTCCAGTTAAGTTAATAATTGGA

GATAAAGAGATATTTGGAATATCAAGAGGTATAGATAAGCAAGGAGCATTATTATTAGAGCAAGATGGAGTAATTAAACCATGGA
TGGGAGGTGAGATAAGTTTACGTAGTGCAGAGAAGGAATTCTCACGTGCTGATTACCCATACGATGTACCAGATTATGCTGGTT
ACCCATATGACGTACCCGATTACGCAGGTTACCCCTACGATGTCCCCGATTACGCATAATCTAGAGCGCGC

miniTurbo

Ordered gene:
ACTAGTGGAGGTAGTGGTGGAAGTCCAAAGAAGAAGAGAAAGGTAGATCCAAAGAAGAAAAGGAAAGTTGATCCAAAGAAAAA
GCGTAAAGTAGCTAGCATTCCATTATTAAATGCTAAGCAAATATTAGGTCAATTAGATGGTGGATCTGTTGCTGTATTACCAGTT
GTAGATAGTACTAATCAATACTTATTAGATAGAATAGGTGAGTTGAAATCAGGAGATGCTTGTATAGCAGAATATCAACAAGCAG
GACGTGGATCAAGAGGACGTAAGTGGTTCTCACCATTCGGAGCAAATTTATACTTAAGTATGTTCTGGCGTTTGAAACGTGGAC
CAGCAGCTATTGGTTTAGGACCAGTTATAGGTATAGTTATGGCAGAGGCTTTACGTAAGTTAGGAGCTGATAAAGTTCGTGTTAA
GTGGCCAAATGATTTATACTTACAAGATCGTAAATTAGCAGGTATATTAGTAGAATTAGCAGGAATTACAGGAGATGCAGCTCAA
ATAGTAATTGGAGCAGGTATTAATGTAGCAATGCGTAGAGTTGAAGAGTCAGTAGTTAATCAAGGTTGGATTACATTACAAGAGG
CTGGAATTAATTTAGATCGTAATACATTAGCTGCAATGTTAATTAGAGAATTAAGAGCTGCATTAGAATTATTCGAGCAAGAGGGT
TTAGCACCATACTTATCTCGATGGGAGAAGTTAGATAATTTCATAAATCGTCCAGTTAAGTTAATAATTGGAGATAAAGAGATATT
TGGAATATCAAGAGGTATAGATAAGCAAGGAGCATTATTATTAGAGCAAGATGGAGTAATTAAACCATGGATGGGAGGTGAGAT
AAGTTTACGTAGTGCAGAGAAGGAATTCTCACGTGCTGATTACCCATACGATGTACCAGATTATGCTGGTTACCCATATGACGTA
CCCGATTACGCAGGTTACCCCTACGATGTCCCCGATTACGCATAATCTAGAGCGCGG

Supplement 2: Primers

See attached file Supplement_2_primers.

Supplement 3: Mass spectrometry results

See attached file Supplement_3_pulldownresults.